CHAPTER 3

The Flow Properties of Blood

3.1 Blood Rheology: An Outline

Blood is a marvelous fluid that nurtures life, contains many enzymes and hormones, and transports oxygen and carbon dioxide between the lungs and the cells of the tissues. We can leave the study of most of these important functions of blood to hematologists, biochemists, and pathological chemists. For biomechanics the most important information we need is the constitutive equation.

Human blood is a suspension of cells in an aqueous solution of electrolytes and nonelectrolytes. By centrifugation, the blood is separated into *plasma* and *cells*. The plasma is about 90% water by weight, 7% plasma protein, 1% inorganic substances, and 1% other organic substances. The cellular contents are essentially all *erythrocytes*, or *red cells*, with *white cells* of various categories making up less than 1/600th of the total cellular volume, and *platelets* less than 1/800th of the cellular volume. Normally, the red cells occupy about 50% of the blood volume. They are small, and number about 5 million/mm^3. The normal white cell count is considered to be from 5000 to 8000/mm^3, and platelets from 250 000 to 300 000/mm^3. Human red cells are disk shaped, with a diameter of 7.6 μm and thickness 2.8 μm. White cells are more rounded and there are many types. Platelets are much smaller and have a diameter of about 2.5 μm.

If the blood is allowed to clot, a straw-colored fluid called *serum* appears in the plasma when the clot spontaneously contracts. Serum is similar to plasma in composition, but with one important colloidal protein, *fibrinogen*, removed while forming the clot. Most of the platelets are enmeshed in the clot.

The specific gravity of red cells is about 1.10; that of plasma is 1.03. When plasma was tested in a viscometer, it was found to behave like a Newtonian viscous fluid (Merrill et al., 1965), with a coefficient of viscosity about 1.2 cP

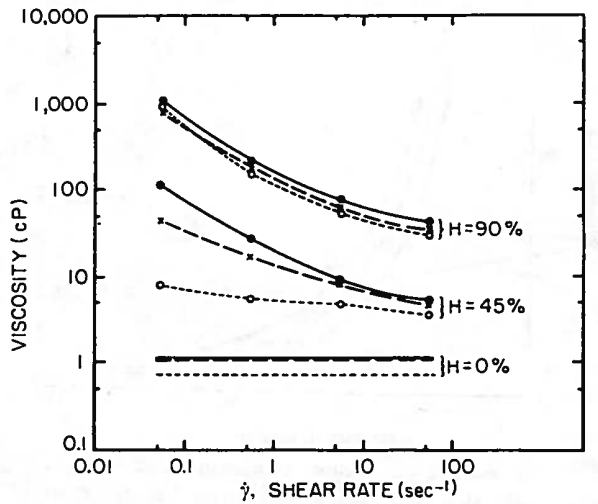

Figure 3.1:1 The viscosity-shear rate relations in whole blood (•—•), defibrinated blood (× --- ×), and washed cells in Ringer soluion (o---o), at 45% and 90% red cell volume concentrations. From Chien et al. (1966), by permission.

(Gregersen et al., 1967; Chien et al., 1966, 1971). When whole blood was tested in a viscometer, its non-Newtonian character was revealed. Figure 3.1:1 shows the variation of the viscosity of blood with the strain rate when blood is tested in a Couette-flow viscometer whose gap width is much larger than the diameter of the individual red cells. For the curves in Fig. 3.1:1, the shear rate $\dot{\gamma}$ is defined as the relative velocity of the walls divided by the width of the gap. The viscosity of blood varies with the *hematocrit*, H, the percentage of the total volume of blood occupied by the cells. It varies also with temperature (see Fig. 3.1:2) and with disease state, if any.

There is a question about what happens to the blood viscosity when the strain rate is reduced to zero. Cokelet et al. (1963) insist that the blood has a finite yield stress. They say that at a vanishing shear rate the blood behaves like an elastic solid. They deduced this conclusion on the basis that their torque measuring device had a rapid response, and could be used to measure transient effects. They studied the time history of the torque after the rotating bob had been stopped suddenly, and compared the transient response for blood with that for a clay suspension, which is known to have a finite yield stress. They showed that the values deduced from this experiment agreed within a few percent with those obtained by extrapolation of the Casson plot as shown in Fig. 3.1:3. Merrill et al. (1965a) also used a capillary viscometer to see if blood in a capillary could maintain a pressure difference across the tube ends without any detectable fluid flow. Such a pressure difference was detected and found to agree with the yield stress determined by Cokelet's method.

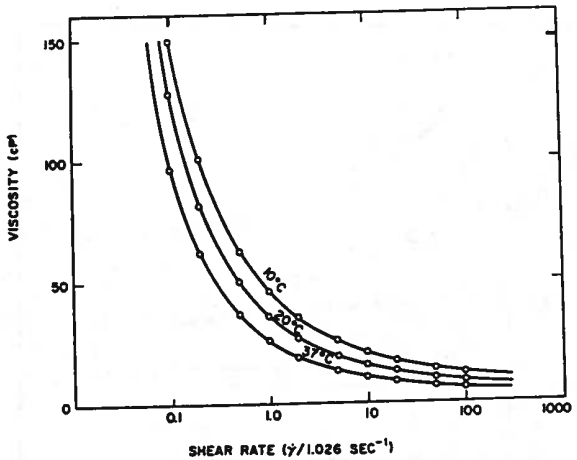

Figure 3.1:2 The variation of the viscosity of human blood with shear rate $\dot{\gamma}$ and temperature for a male donor, containing acid citrate dextrose, reconstituted from plasma and red cells to the original hematocrit of 44.8. From Merrill et al. (1963a, p. 206), by permission.

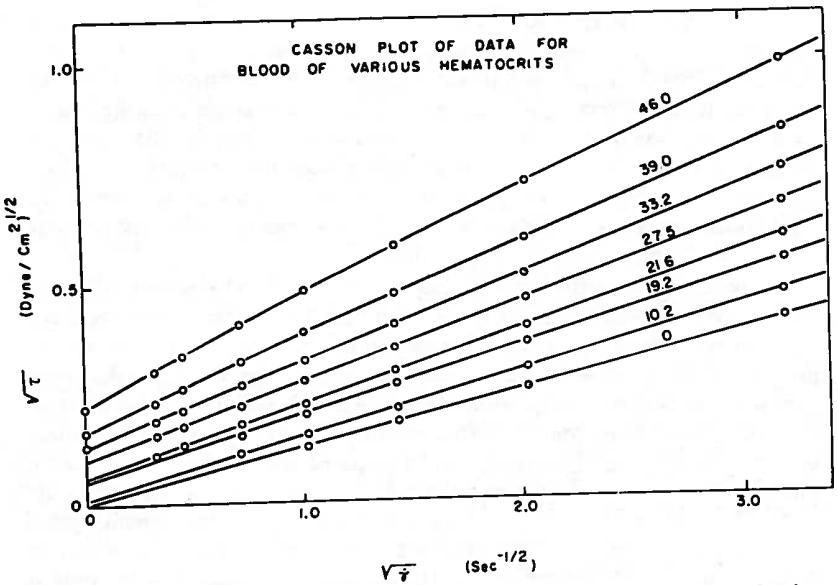

Figure 3.1:3 Casson plot of very low shear rate data for a sample of human blood at a temperature of 25°C. Range of linearity decreases as the hematocrit increases. Plasma is Newtonian. Data from Cokelet et al. (1963), by permission.

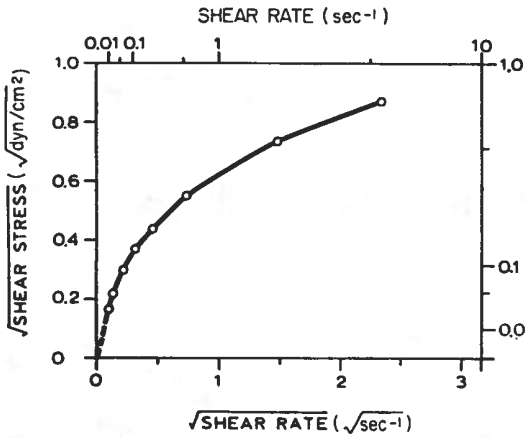

Figure 3.1:4 Casson plot for whole blood at a hematocrit of 51.7 (temp. = 37°C), according to Chien et al. (1966), by permission.

It must be understood that by "existence" of a yield stress is meant that no sensible flow can be detected in a fluid under a shearing stress in a finite interval of time (say, 15 min). The difficulty of determining the yield stress of blood as $\dot{\gamma} \to 0$ is compounded by the fact that an experiment for very small shear rate is necessarily a transient one if that experiment is to be executed in a finite interval of time. For blood the analysis is further complicated by the migration of red cells away from the walls of the viscometer when $\dot{\gamma}$ is smaller than about $1\ s^{-1}$. Cokelet's analysis takes these factors into account, and requires considerable manipulation of the raw data (see Cokelet, 1972). If the maximum transient shear stress reached after the start of an experiment at constant shear rate is plotted directly with respect to the nominal shear rate, the result appears as shown in Fig. 3.1:4 by Chien et al. (1966). The differences between the plots of Figs. 3.1:3 and 3.1:4 are caused mainly by the data analysis procedures, and partly reflect the dynamics of the instrument as well as that of the blood state.

The data of Cokelet et al. for a small shear rate, say $\dot{\gamma} < 10\ s^{-1}$, and for hematocrit less than 40%, can be described approximately by Casson's (1959) equation

$$\sqrt{\tau} = \sqrt{\tau_y} + \sqrt{\eta\dot{\gamma}}, \tag{1}$$

where τ is the shear stress, $\dot{\gamma}$ is the shear strain rate, τ_y is a constant that is interpreted as the yield stress in shear, and η is a constant. The fitting of this equation to experimental data can be seen in Fig. 3.1:3, from which it is clear that for hematocrit below 33% the experimental data points fall quite accurately on straight lines. For higher hematocrit (39% and above), deviations from straight lines are more evident. The yield stress τ_y given by Merrill

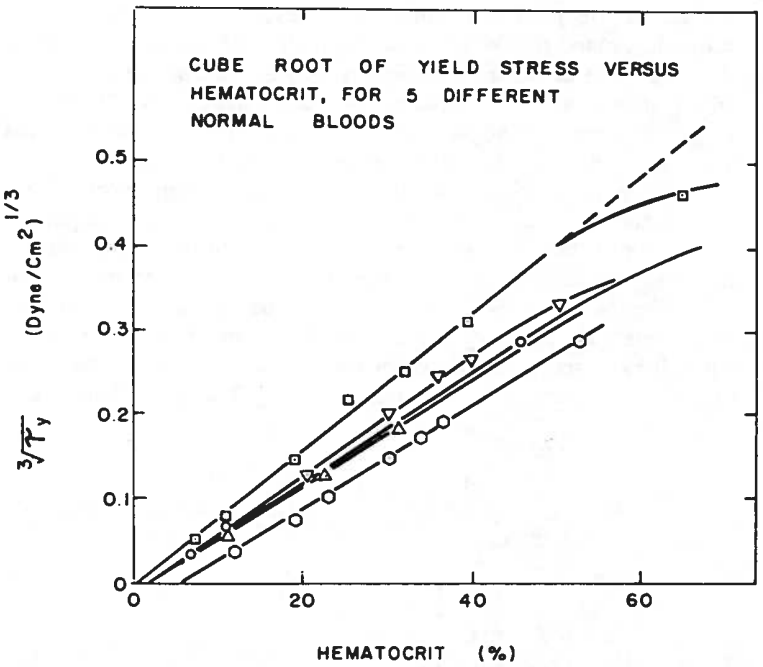

Figure 3.1:5 Variation of the yield stress of blood from five different donors with hematocrit. Tests on samples with hematocrits less than the applicable abscissa intercept showed no yield stress. From Merrill et al. (1963a), by permission. ACD was used as anticoagulant.

et al. (1963) is shown in Fig. 3.1:5. Note that τ_y is very small: of the order of 0.05 dyn/cm^2, and is almost independent of the temperature in the range 10–37°C. τ_y is markedly influenced by the macromolecular composition of the suspending fluid. A suspension of red cells in saline plus albumin has zero yield stress; a suspension of red cells in plasma containing fibrinogen has a finite yield stress.

At high shear rate, whole blood behaves like a Newtonian fluid with a constant coefficient of viscosity, as is seen in Fig. 3.1:1. In other words, for sufficiently large values of $\dot{\gamma}$ we have

$$\tau = \mu\dot{\gamma} \quad \text{or} \quad \sqrt{\tau} = \sqrt{\mu}\sqrt{\dot{\gamma}}, \qquad \mu = \text{const.} \tag{2}$$

As the shear rate $\dot{\gamma}$ increases from 0 to a high value, there is a transition region in which the stress–strain rate relation changes from that described by Eq. (1) to that described by Eq. (2). This is illustrated in Fig. 3.1:6, with data from Brooks et al. (1970). The part of the data to the right of the dashed curve belongs to the Newtonian region, described by Eq. (2); straight regression lines pass through the origin. The part to the left of the dashed curve

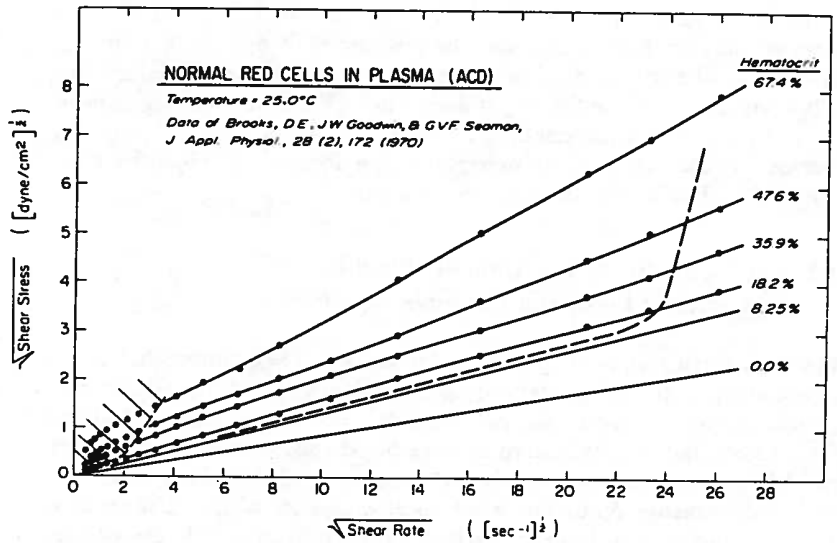

Figure 3.1:6 Casson plot of higher shear rate rheological data for a blood with ACD anticoagulant. The actual data points for plasma and the 8.25% hematocirt red cell suspension are not shown for clarity; these fluids appear to be Newtonian. Viscometer surfaces were smooth. From Cokelet (1972), by permission.

is the non-Newtonian region. The range of validity of Eq. (1) is smaller for higher hematocrit, and the transition region from Eq. (1) to Eq. (2) is larger for higher hematocrit. For hematocrit below 40% at 37°C, Eqs. (1) and (2) can be assumed to merge smoothly.

This outline shows the major features of blood flow in a viscometer of the Couette-flow type. The width of the channel in which blood flows in these testing machines is much larger than the diameter of the red blood cells. The blood is considered as a *homogeneous fluid*. This is a reasonable way to look at the blood when we analyze blood flow in large blood vessels. But all our blood vessels are not so large. In the human body there are about 10^{10} blood vessels whose diameter is about the same as that of the red blood cells, ranging from 4 to 10 μm. These are called the *capillary blood vessels*. When blood flows in capillary blood vessels, the red cells have to be squeezed and deformed, and move in single file. In this case, then, it would be more useful to consider blood as a *nonhomogeneous* fluid, of at least two phases, one phase being the blood cells, the other being the plasma. Between large arteries and veins and the capillaries there are blood vessel of varying diameters. At what level can we regard blood as homogeneous? This is a question whose answer depends on the fluid mechanical features that one wishes to examine. Flow of blood in microvessels has many unique features, which will be discussed in Chapter 5.

In the present chapter, we shall first put the experimental results in a form suitable for further analysis. The problem of blood flow in a circular cylindrical tube will be discussed. We shall then turn to the question why blood viscosity behaves the way it does. Through this kind of examination, we will gain some understanding of blood rheology in states of health or disease. We shall conclude this chapter with a discussion of blood coagulation and medical applications of blood rheology.

3.2 The Constitutive Equation of Blood Based on Viscometric Data and Casson's Equation

Blood is a mixture of blood plasma and blood cells. The mixture, when tested in viscometers whose characteristic dimension is much larger than the characteristic size of the blood cells, yields the data outlined in Sec. 3.1. In these viscometers, and, by implication, in large blood vessels whose diameters are much larger than the characteristic size of the blood cells, blood may be treated as a homogeneous fluid. The mechanical properties of the mixture as a homogeneous fluid can be described by a constitutive equation. In this section, such a constitutive equation based on the viscometric data outlined in Sec. 3.1 is formulated as an *isotropic* and *incompressible fluid*. The assumption of isotropy is motivated by the idea that when the shear stress and shear strain rate are zero, the blood cells have no preferred orientation. The assumption of incompressibility is based on the fact that, in the range of pressures concerned in physiology, the mass densities of the plasma, the cells, and the mixture as a whole are unaffected by the pressure.

The rheology of blood revealed in Sec. 3.1 differs from that of a Newtonian fluid only in the fact that the coefficient of viscosity is not a constant. The constitutive equation of an isotropic incompressible Newtonian fluid is

$$\sigma_{ij} = -p\delta_{ij} + 2\mu V_{ij}, \tag{1}$$

where

$$V_{ij} = \frac{1}{2}\left(\frac{\partial u_i}{\partial x_j} + \frac{\partial u_j}{\partial x_i}\right), \qquad V_{ii} = V_{11} + V_{22} + V_{33} = 0. \tag{2}$$

Here σ_{ij} is the stress tensor, V_{ij} is the strain-rate tensor, u_i is the velocity component, δ_{ij} is the isotropic tensor or Kronecker delta, p is the hydrostatic pressure, and μ is a constant called the *coefficient of viscosity*. The indices i, j range over 1, 2, 3, and the components of the tensors and vectors are referred to a set of rectangular cartesian coordinates x_1, x_2, x_3. The summation convention is used, so that a repetition of an index means summation over the index, e.g., $V_{ii} = V_{11} + V_{22} + V_{33}$. Note the factor $\frac{1}{2}$ in our definition of strain rate in Eq. (2). This definition makes V_{ij} a tensor. In older books, shear rate is defined as twice this value. Thus $\dot{\gamma}$ of Fig. 3.1:1 is equal to $2V_{12}$ if the coordinate axes x_1, x_2 point at directions parallel and perpendicular to the wall, respectively.

Blood does not obey Eq. (1) because μ is not a constant. μ varies with the strain rate. Thus blood is said to be *non-Newtonian*. Similar experiments do verify, however, that *normal plasma alone is Newtonian*. Therefore the non-Newtonian feature of whole blood comes from the cellular bodies in the blood.

How can we generalize the Newtonian equation (1) to accommodate the non-Newtonian behavior of blood? What guidance do we have?

The most important principle we learned from continuum mechanics is that any equation must be tensorially correct, i.e., every term in an equation must be a tensor of the same rank. Thus, if we decide to try an equation of the type of Eq. (1) for blood, under the assumption that its mechanical behavior is isotropic, then μ is a scalar, i.e., μ must be a scalar function of the strain rate tensor V_{ij}. Now, V_{ij} is a symmetric tensor of rank 2 in three dimensions. It has three invariants which are scalars. Hence the coefficient of viscosity μ must be a function of the invariants of V_{ij}. These invariants are:

$$\begin{aligned} I_1 &= V_{11} + V_{22} + V_{33}, \\ I_2 &= \begin{vmatrix} V_{11} & V_{12} \\ V_{21} & V_{22} \end{vmatrix} + \begin{vmatrix} V_{22} & V_{23} \\ V_{32} & V_{33} \end{vmatrix} + \begin{vmatrix} V_{33} & V_{31} \\ V_{13} & V_{11} \end{vmatrix}, \\ I_3 &= \begin{vmatrix} V_{11} & V_{12} & V_{13} \\ V_{21} & V_{22} & V_{23} \\ V_{31} & V_{32} & V_{33} \end{vmatrix}. \end{aligned} \tag{3}$$

See the author's *First Course*, 3rd edn., Chapter 5. But we have assumed blood to be incompressible; hence I_1 vanishes. But when $I_1 = 0$, I_2 is negative valued, and it is more convenient to use a positive-valued invariant J_2 defined by

$$J_2 = \tfrac{1}{3}I_1^2 - I_2 = \tfrac{1}{2}V_{ij}V_{ij}. \tag{4}$$

Hence μ must be a function of J_2 and I_3. From Eq. (4) it is seen that J_2 is directly related to the shear strain rate. For example, if V_{12} is the only non-vanishing component of shear rate, then $J_2 = V_{12}^2$. From experiments described in Sec. 3.1 we know that the blood viscosity depends on the shear rate, hence on J_2. Whether it depends on I_3 or not is unknown because in most viscometric flows (e.g., Couette, Poiseuille, and cone-plate flows, see Sec. 2.14) I_3 is zero. Thus, we assume that μ is a function of J_2 and propose the following constitutive equation for blood when it flows:

$$\sigma_{ij} = -p\delta_{ij} + 2\mu(J_2)V_{ij}. \tag{5}$$

Let us now compare this proposal with experimental results. For the simple shear flow shown in Fig. 2.7:1 in Sec. 2.7, we have the shear rate

$$\dot{\gamma} = \frac{v}{h} = 2 \cdot \frac{1}{2}\left(\frac{\partial v_1}{\partial x_2} + \frac{\partial v_2}{\partial x_1}\right) = 2V_{12}. \tag{6}$$

(Note the factor of 2 due to the difference in the old and the tensorial de-

finition of strain rate as remarked previously.) In this case, all other components V_{ij} vanish, and

$$J_2 = V_{12}^2, \tag{7}$$

so that from Eq. (6),

$$|\dot{\gamma}| = 2\sqrt{J_2}, \tag{8}$$

whereas from Eq. (5), we have the shear stress

$$\sigma_{12} = 2\mu(J_2)V_{12} = \mu\dot{\gamma}. \tag{9}$$

It is shown in Sec. 3.1 that in steady flow in larger vessels, the experimental results may be expressed in Casson's equation, Eq. (1) of Sec. 3.1,

$$\sigma_{12} = [\sqrt{\tau_y} + \sqrt{\eta|\dot{\gamma}|}]^2 \tag{10}$$

in a wide range of $\dot{\gamma}$. Comparing Eqs. (9) and (10), we see that

$$\mu = \frac{[\sqrt{\tau_y} + \sqrt{\eta|\dot{\gamma}|}]^2}{|\dot{\gamma}|}. \tag{11}$$

Thus, we conclude that the constitutive equation for blood is, in the range of $\dot{\gamma}$ when blood flows,

$$\sigma_{ij} = -p\delta_{ij} + 2\mu(J_2)V_{ij}, \tag{12a}$$

where

$$\mu(J_2) = [(\eta^2 J_2)^{1/4} + 2^{-1/2}\tau_y^{1/2}]^2 J_2^{-1/2}. \tag{12b}$$

Equation (12) is valid when $J_2 \neq 0$ and sufficiently small. On the other hand, when J_2 is sufficiently large, the experimental results reduce to the simple statement that μ = constant, so that Eq. (1) applies. The point of transition from Eqs. (12a,b) to the Newtonian equation, μ = constant, depends on the hematocrit, H (the volume fraction of red blood cells in whole blood). For normal blood with a low hematocrit, $H = 8.25\%$, μ was found to be constant over the entire range of shear rate from 0.1 to 1000 s^{-1}. When $H = 18\%$, the blood appears to be Newtonian when $\dot{\gamma} > 600\ s^{-1}$, but obeys Eq. (12) for smaller $\dot{\gamma}$. For higher H the transition point increases to $\dot{\gamma} \cong 700\ s^{-1}$. See Fig. 3.1:6.

The flow rule must be supplemented by another stress–strain relation when the blood is not flowing, i.e., when $V_{ij} = 0$. We know so little about the behavior of blood in this condition, however, that only a hypothetical constitutive equation can be proposed. A Hooke's law, for example, may be suggested when there is no flow, because the stress and strain are both very small. (The "yielding stress," τ_y, in Eq. (11) or (12), is only of the order of 0.05 dyn/cm^2. The weight of a layer of water 1 mm thick, spreading over 1 cm^2, produces a compressive stress of 100 dyn/cm^2!) For a complete formulation, we need another condition, the "yielding condition," to define at what stress level flow must occur. In the theory of plasticity, the yielding condition is often

stated in terms of the second invariant of the stress deviation, defined as

$$J_2' = \tfrac{1}{2}\sigma_{ij}'\sigma_{ij}', \tag{13}$$

where

$$\sigma_{ij}' = \sigma_{ij} - \tfrac{1}{3}\sigma_{kk}\delta_{ij}. \tag{14}$$

Flow or yielding occurs when J_2' exceeds a certain number K. Thus:

$$V_{ij} = \begin{cases} 0 & \text{if } J_2' < K, \\ \dfrac{1}{2\mu}\sigma_{ij}' & \text{if } J_2' \geq K. \end{cases} \tag{15}$$

The stress–strain law when there is no flow, the yielding condition, and the flow rule together describe the mechanical behavior of the blood.

3.2.1 Other Aspects of Blood Rheology

Actually the rheological properties of blood are more complex than what is portrayed above. If blood is tested dynamically, it can be made to reveal all features of viscoelasticity. Furthermore, the viscoelastic characteristics of blood change with the level of strain and strain history; hence it is *thixotropic*. These complex properties are probably unimportant in normal circulatory physiology, but can be significant when one tries to use blood rheology as a basis of clinical applications to diagnosis of diseases, pathology, or biochemical studies.

3.2.2 Why Do We Need the General Constitutive Equation?

We have obtained, with some effort in theoretical reasoning, a constitutive equation for blood that is consistent with our experimental knowledge. Why is this complicated constitutive equation needed? The answer is that although the simple Casson equation, Eq. (1) of Sec. 3.1, suffices in the analysis of simple problems in which the strain rate tensor can be calculated a priori (without using the constitutive equation), in more complex problems it is insufficient. Casson's equation is all we need in analyzing Poiseuille and Couette flows, for which the shear stress and strain distributions are known from statics and kinematics. But if we wish to analyze the flow of blood at the point of bifurcation of an artery into two branches, or the flow through a stenosis, or the flow in aortic sinus, etc., the stress and strain rate distributions are not known. To analyze these problems, it is necessary to write down the general equations of motion based on an appropriate constitutive equation and solve them. For these problems the general constitutive equation is necessary.

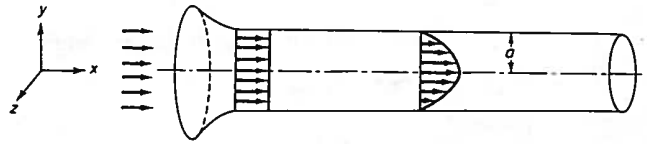

Figure 3.3:1 Velocity profiles in a steady laminar flow into a circular cylindrical tube.

3.3 Laminar Flow of Blood in a Tube

Let us consider the flow of blood in a circular cylindrical tube. We shall assume the flow to be *laminar*, that is, *not turbulent*. We shall also assume that the tube is long and the flow is steady, so that the conditions of flow change neither with the distance along the tube, nor with the time. Under these assumptions we can analyze the flow with a simple ad hoc approach, which is presented below.

We shall use polar coordinates for this problem. The polar axis coincides with the axis of the cylinder. See Fig. 3.3:1. The flow obeys Navier–Stokes equations of motion of an incompressible fluid. The boundary condition is that blood adheres to the tube wall (the so-called *no-slip* condition). Since the boundary condition is axisymmetric, the flow is also axisymmetric and the only nonvanishing component of velocity is $u(r)$ in the axial direction; $u(r)$ is a function of r alone, and not of x. Isolate a cylindrical body of fluid of radius r and unit length in the axial direction, as shown in Fig. 3.3:2(a). This body is subjected to a pressure p_1 on the left-hand end, p_2 on the right-hand end, and shear stress τ on the circumferential surface. Since $p_1 - p_2 = -1 \cdot (dp/dx)$ acts on an area πr^2, and τ acts on an area $1 \cdot 2\pi r$, we have, for equilibrium, the balance of forces

$$\tau \cdot 2\pi r = -\pi r^2 \frac{dp}{dx},$$

or

$$\tau = -\frac{r}{2}\frac{dp}{dx} \qquad \text{(Stokes, 1851).} \tag{1}$$

This important result is shown in Fig. 3.3:2(b).

Now we must introduce a constitutive equation that relates the shear stress τ to the velocity gradient. Let us first consider a Newtonian fluid.

3.3.1 A Newtonian Fluid

By the definition of Newtonian viscosity, we have

$$\tau = -\mu \frac{du}{dr}. \tag{2}$$

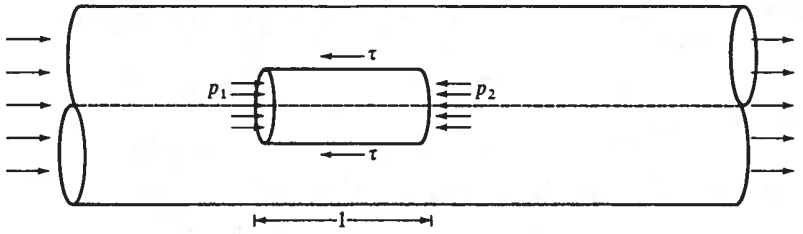

(a)

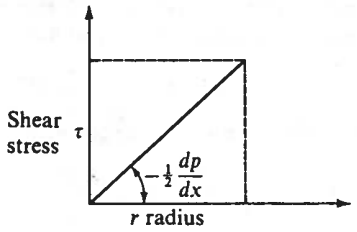

(b)

Figure 3.3:2 Steady flow in a long circular cylindrical pipe. (a) A free-body diagram of a centrally located element on which pressure and shear stresses act. (b) Relationship between the shear stress τ and the radial distance r from the axis of symmetry.

A substitution of Eq. (2) into Eq. (1) yields

$$\frac{du}{dr} = \frac{r}{2\mu}\frac{dp}{dx}. \tag{3}$$

Since the left-hand side is a function of r, the right-hand side must be also. Hence dp/dx cannot be a function of x. But since the fluid does not move in the radial direction, the pressures in the radial direction must be balanced, and p cannot vary with r. Hence the pressure gradient dp/dx must be a constant. Therefore, we can integrate Eq. (3) to obtain

$$u = \frac{r^2}{4\mu}\frac{dp}{dx} + B, \tag{4}$$

where B is an integration constant. B can be determined by the boundary condition of no-slip:

$$u = 0 \qquad \text{when} \quad r = a. \tag{5}$$

Combining Eqs. (4) and (5) yields the solution

$$u = -\frac{1}{4\mu}(a^2 - r^2)\frac{dp}{dx}, \tag{6}$$

which shows that the velocity profile is a parabola, as sketched in Fig. 3.3:1.

The *rate of flow* through the tube can be obtained by integrating velocity times area over the tube cross section:

$$\dot{Q} = 2\pi \int_0^a ur\,dr. \tag{7}$$

On substituting Eq. (6) into Eq. (7), we obtain the well-known formula

$$\dot{Q} = -\frac{\pi a^4}{8\mu}\frac{dp}{dx}. \tag{8}$$

A division of the rate of flow by the cross-sectional area of the tube yields the mean velocity of flow,

$$u_m = -\frac{a^2}{8\mu}\frac{dp}{dx}. \tag{9}$$

3.3.2 Blood, with Viscosity Described by Casson's Equation

If we compute the shear strain rate of the fluid at the tube wall, using the formulas obtained above for a Newtonian fluid, we obtain

$$\left.\frac{du}{dr}\right|_{r=a} = \frac{1}{2}\frac{a}{\mu}\frac{dp}{dx} \qquad \text{from Eq. (3) or (6),} \tag{10}$$

or

$$\left.\frac{du}{dr}\right|_{r=a} = -\frac{4u_m}{a} \qquad \text{from Eqs. (3) and (9).} \tag{11}$$

If physiological data on u_m, a, μ, and dp/dx are substituted into Eqs. (10) and (11), we find that $\dot{\gamma}$ ($= -du/dr$ at $r = a$) ranges from 100 to 2000 sec^{-1} in large and small arteries, and 20 to 200 sec^{-1} in large and small veins. Thus in the neighborhood of the blood vessel wall, the shear rate is high enough for the Newtonian assumption to be valid for normal blood. Toward the center of the tube, however, the shear gradient tends to zero, and the non-Newtonian feature of the blood will become more evident.

Let us assume that the blood is governed by Casson's equation, Eq. (1) of Sec. 3.1 or Eq. (12) of Sec. 3.2. We assume that the flow is laminar, uniaxial, axisymmetric, and without entrance effect (far away from the ends of the tube).

Equation (1) is valid for any fluid, hence for blood. The shear stress acting on any cylindrical surface ($r = \text{const.}$) is proportional to r, as shown in Fig. 3.3:2 and reproduced in Fig. 3.3:3. On the wall, the shear stress is τ_w. At a certain point on the stress axis it is τ_y, the yield stress. This corresponds to a radius r_c, shown on the horizontal axis. If the shear stress is smaller than the yield stress, that is, $\tau < \tau_y$ or $r < r_c$, the blood will not flow. If it moves at all it would have to move like a rigid body. Therefore, the velocity profile depends on the relative magnitude of τ_y and τ_w. Now, by Eq. (1),

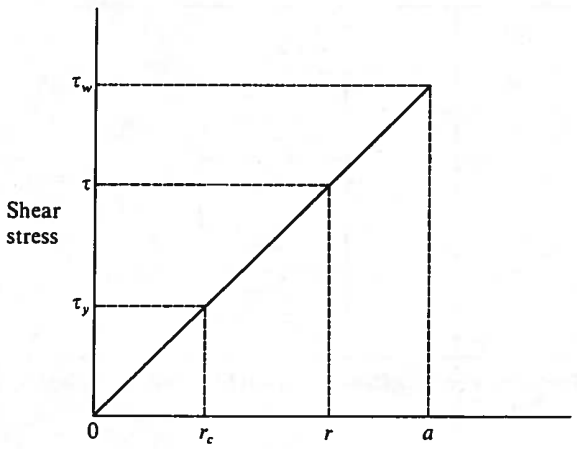

Figure 3.3:3 The relationship between shear stress and radial distance in a steady pipe flow. The shear stress reaches the yields stress of blood τ_y at radial distance r_c.

$$\tau_w = -\frac{a}{2}\frac{dp}{dx}, \qquad \tau_y = -\frac{r_c}{2}\frac{dp}{dx}. \tag{12}$$

Therefore, if $\tau_y > \tau_w$, i.e., $r_c > a$, then there is no flow:

$$u = 0 \qquad \text{when} \quad -\frac{dp}{dx} < \frac{2\tau_y}{a}. \tag{13}$$

If $\tau_y < \tau_w$, i.e., $r_c < a$, or

$$-\frac{dp}{dx} > \frac{2\tau_y}{a}, \tag{14}$$

then the velocity profile of the flow will be like that sketched in Fig. 3.3:4. In the core, $r < r_c$, the profile is flat. Between r_c and a, Casson's equation applies:

$$\sqrt{\tau} = \sqrt{\eta}\sqrt{\dot{\gamma}} + \sqrt{\tau_y}, \tag{15}$$

η is called *Casson's coefficient of viscosity*. Taking the square root of Eq. (1) and using Eq. (15), we obtain

$$\sqrt{-\frac{r}{2}\frac{dp}{dx}} = \sqrt{\tau_y} + \sqrt{\eta}\sqrt{\dot{\gamma}}. \tag{16}$$

Solving for $\dot{\gamma}$, we have

$$-\frac{du}{dr} = \dot{\gamma} = \frac{1}{\eta}\left(\sqrt{-\frac{r}{2}\frac{dp}{dx}} - \sqrt{\tau_y}\right)^2. \tag{17}$$

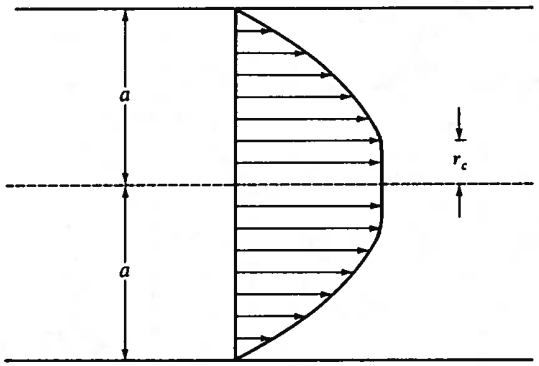

Figure 3.3:4 The velocity profile of laminar flow of blood in a long circular cylindrical pipe.

Integrating this equation and using the no-slip boundary condition $u = 0$ when $r = a$, we have

$$-\int_r^a \frac{du}{dr}\,dr = u|_r - u|_a = \frac{1}{\eta}\int_r^a \left(\sqrt{-\frac{r}{2}\frac{dp}{dx}} - \sqrt{\tau_y}\right)^2 dr, \tag{18}$$

or

$$u = -\frac{1}{4\eta}\frac{dp}{dx}\left[a^2 - r^2 - \tfrac{8}{3}r_c^{1/2}(a^{3/2} - r^{3/2}) + 2r_c(a - r)\right] \quad \text{for } (r_c \le r \le a). \tag{19}$$

At $r = r_c$, the velocity u becomes the core velocity u_c:

$$\begin{aligned} u_c &= -\frac{1}{4\eta}\frac{dp}{dx}\left(a^2 - \tfrac{8}{3}r_c^{1/2}a^{3/2} + 2r_c a - \tfrac{1}{3}r_c^2\right) \\ &= -\frac{1}{4\eta}\frac{dp}{dx}(\sqrt{a} - \sqrt{r_c})^3(\sqrt{a} + \tfrac{1}{3}\sqrt{r_c}). \end{aligned} \tag{20}$$

And for all values of r between 0 and r_c,

$$u = u_c. \tag{21}$$

The velocity distribution is given by Eqs. (19) and (21) if $r_c < a$, i.e., if Eq. (14) applies; whereas the flow is zero if the inequality sign in Eq. (14) is reversed.

We can now find the rate of volume flow by an integration:

$$\dot{Q} = 2\pi\int_0^a ur\,dr. \tag{22}$$

Using Eqs. (13), (19), and (21) for appropriate ranges of pressure gradient and radius, we obtain

$$\dot{Q} = \frac{\pi a^4}{8\eta}\left[-\frac{dp}{dx} - \frac{16}{7}\left(\frac{2\tau_y}{a}\right)^{1/2}\left(-\frac{dp}{dx}\right)^{1/2} + \frac{4}{3}\left(\frac{2\tau_y}{a}\right) - \frac{1}{21}\left(\frac{2\tau_y}{a}\right)^4\left(-\frac{dp}{dx}\right)^{-3}\right] \tag{23}$$

if $dp/dx > (2\tau_y/a)$; whereas

$$\dot{Q} = 0 \qquad \text{if} \quad -\frac{dp}{dx} < \frac{2\tau_y}{a}. \tag{24}$$

If we introduce the notation

$$\xi = \left(\frac{2\tau_y}{a}\right)\left(-\frac{dp}{dx}\right)^{-1}, \tag{25}$$

then Eq. (23) can be written as

$$\dot{Q} = -\frac{\pi a^4}{8\eta}\frac{dp}{dx}F(\xi), \tag{26}$$

where

$$F(\xi) = 1 - \frac{16}{7}\xi^{1/2} + \frac{4}{3}\xi - \frac{1}{21}\xi^4. \tag{27}$$

Equation (26) is similar to Poiseuille's law, but with a modifying factor $F(\xi)$. These results were obtained by S. Oka (1965, 1974). Figure 3.3:5 gives Oka's graph of $F(\xi)$ vs. ξ. It is seen that the flow rate decreases rapidly with increasing ξ. For $\xi > 1$, there is no flow, and $\dot{Q} = 0$. Oka also obtained the interesting result shown in Fig. 3.3:6, that if one plots the square root of $\dot{Q}$ vs. the square root of the pressure gradient, one obtains a curve that resembles the flow vs. shear stress curve of a Bingham plastic material (see Problem 3.17, p. 97). Taking the square root on both sides of Eq. (26), expanding the square root of $F(\xi)$ in a power series of $\xi^{1/2}$, and retaining only the first power, one obtains the asymptotic equation

$$\begin{aligned} Q^{1/2} &= \left(\frac{\pi a^4}{8\eta}\right)^{1/2}\left(-\frac{dp}{dx}\right)^{1/2}(1 - \tfrac{8}{7}\xi^{1/2}) \\ &= \left(\frac{\pi a^4}{8\eta}\right)^{1/2}\left[\left(-\frac{dp}{dx}\right)^{1/2} - \tfrac{8}{7}p_c^{1/2}\right], \end{aligned} \tag{28}$$

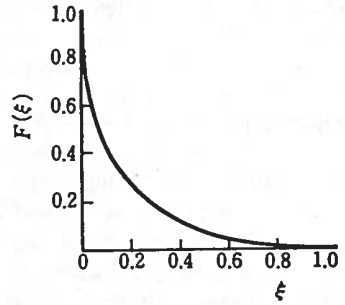

Figure 3.3:5 The function $F(\xi)$ from Eq. (37) of Sec. 3.5, which is the ratio of the flow rate in a tube of a fluid obeying Casson's equation to that of a Newtonian fluid with the same Casson viscosity. The variable ξ is inversely proportional to the pressure gradient; see Eq. (36) of Sec. 3.5. From Oka (1974), by permission.

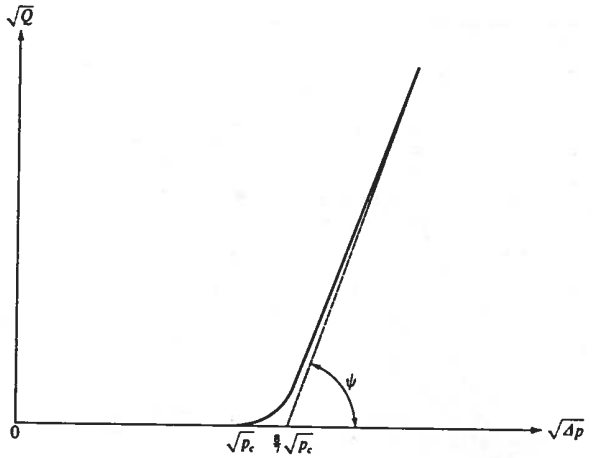

Figure 3.3:6 The relationship between $\sqrt{Q}$ and $\sqrt{\Delta p}$; Q is the flow rate of a fluid obeying Casson's equation, and Δp is the pressure gradient. From Oka (1974), by permission.

where $p_c = 2\tau_y/a$. This is plotted as the dotted line in Fig. 3.3:6. The solid curve is the exact solution. The dotted line is an asymptote whose slope is

$$\tan\psi = \left(\frac{\pi a^4}{8\eta}\right)^{1/2}. \tag{29}$$

These results give complete information on the laminar flow of blood in circular cylindrical tubes.

3.4 Speculation on Why Blood Viscosity Is the Way It Is

Since normal plasma is Newtonian, there is no doubt that the non-Newtonian features of human blood come from blood cells. How the red blood cells move when blood flows is the central issue.

It has been known for a long time (Fahraeus, 1929) that human red blood cells can form aggregates known as rouleaux (Fig. 3.4:1), whose existence depends on the presence of the proteins fibrinogen and globulin in plasma. (Bovine blood does not form rouleaux.) The slower the blood flows, or rather, the smaller the shear rate, the more prevalent are the aggregates. When the shear rate tends to zero, it is speculated that human blood becomes one big aggregate, which then behaves like a solid. A solid may be viscoelastic or viscoplastic. If the blood aggregate behaves as a plastic solid, then a yield stress exists which can be (but does not have to be) identified with the constant τ_y in Casson's equation [Eq. (1) of Sec. 3.1].

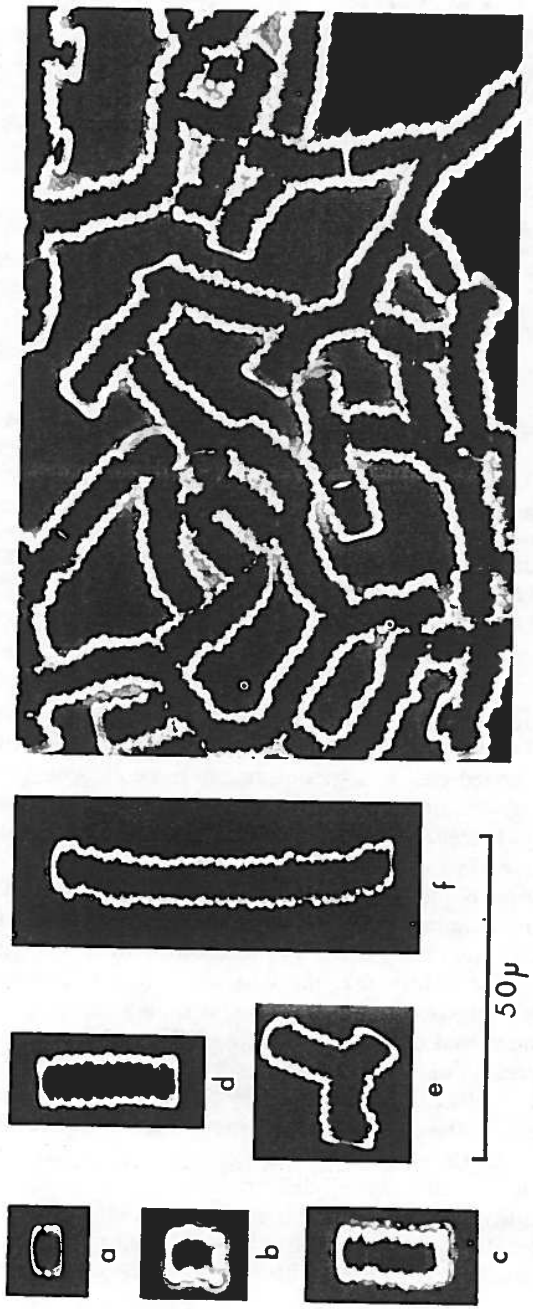

Figure 3.4:1 Rouleaux of human red cells photographed on a microscope slide showing single linear and branched aggregates (left part) and a network (right part). The number of cells in linear array are 2, 4, 9, 15, and 36 in a, b, c, d, and f, respectively. From Goldsmith (1972b), by permission.

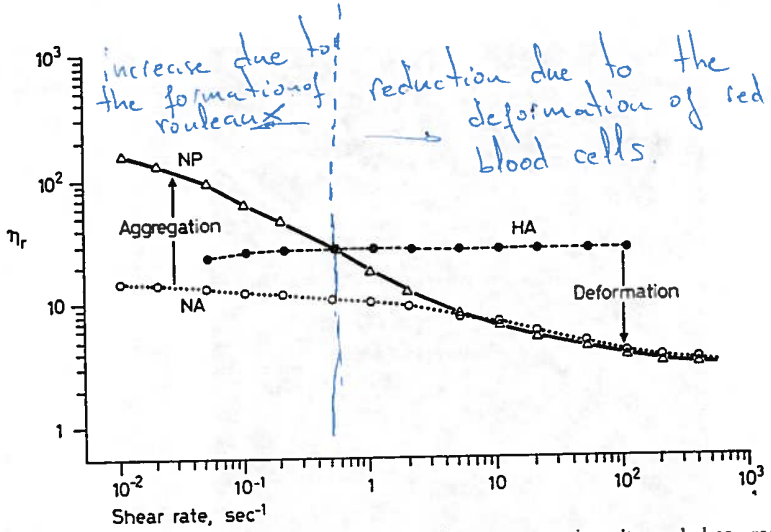

Figure 3.4:2 Logarithmic relation between relative apparent viscosity and shear rate in three types of suspensions, each containing 45% human RBC by volume. Suspending medium (plasma) viscosity = 1.2 cP (= 1.2×10^{-3} N s m^{-2}). NP = Normal RBC in plasma; NA = normal RBC in 11% albumin; HA = hardened RBC in 11% albumin. From Chien (1970), by permission.

When the shear rate increases, blood aggregates tend to be broken up, and the viscosity of blood is reduced. As the shear rate increases further, the deformation of the red cells becomes more and more evident. The cells tend to become elongated and line up with the streamlines. This further reduces the viscosity. The effects of aggregation and deformation of the red cells are well illustrated in Fig. 3.4:2, from Chien (1970). In this figure, the line NP refers to normal blood. The line NA refers to a suspension of normal red blood cells in an albumin-Ringer solution that does not contain fibrinogen and globulins. The tendency toward rouleaux formation was removed in the latter case, and it is seen that the viscosity of the suspension was reduced, even though the viscosity of the albumin-Ringer solution was adjusted to be the same as that of the plasma of the NP case. The third curve, HA, refers to a suspension of hardened red blood cells in the same albumin-Ringer solution. (Red cells can be hardened by adding a little fixing agent such as glutaraldehyde to the solution.) Hence the difference between the NP and NA curves indicates the effect of cell aggregation, whereas that between NA and HA indicates the effect of cell deformation.

The amazing fluidity of human blood is revealed in Fig. 3.4:3, in which the viscosity of blood at a shear rate > 100 s^{-1} (at which particle aggregation ceased to be important) is compared with that of other suspensions and

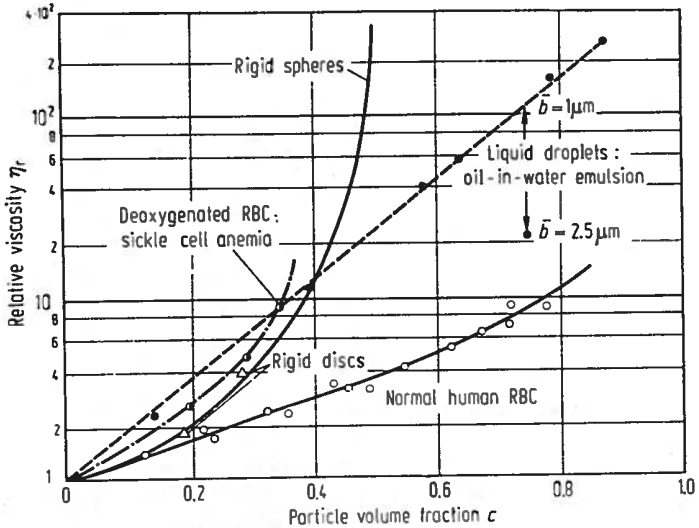

Figure 3.4:3 Relative viscosity of human blood at 25°C as a function of red cell volume fraction, compared to that of suspensions of rigid latex spheres, rigid disks, droplets, and sickled erythrocytes, which are virtually nondeformable. From Goldsmith (1972b), by permission.

emulsions. At 50% concentration, a suspension of rigid spheres will not be able to flow, whereas blood is fluid even at 98% concentration by volume. The much higher viscosity of blood with deoxygenated sickle cells is also shown: it tells us why sickle cell anemia is such a serious disease.

Since in a field of shear flow with a velocity gradient in the y direction the velocity is different at different values of y, any suspended particle of finite dimension in the y direction will tumble while flowing. The tumbling disturbs the flow and requires expenditure of energy, which is revealed in viscosity. If n red cells form a rouleaux, the tumbling of the rouleaux will cause more disturbance than the sum of the disturbances of the n individual red cells. Hence breaking up the rouleaux will reduce the viscosity. Further reduction can be obtained by deformation of the particle. If the particle is a liquid droplet, for example, it can elongate to reduce the dimension in the y direction, thus reducing the disturbance to the flow. A red cell behaves somewhat like a liquid droplet; it is a droplet wrapped in a membrane. These factors explain the reduction of viscosity with increasing shear rate.

Detailed studies of the tumbling and deformation of the red cells and rouleaux in shear flow have been made by Goldsmith and his associates by observing blood flow in tiny circular cylindrical glass tubes having diameters from 65 to 200 μm under a high powered microscope. The tubes lay on a

vertically mounted platform, which was moved mechanically or hydraulically upward as the particles being tracked flowed downward from a syringe reservoir. The cell motion was photographed. Particle behavior at hematocrits $> 10\%$ was studied by using tracer red cells in a transparent suspension of hemolyzed, unpigmented red cells—so-called *ghost cells*. The ghosts were also biconcave in shape, although their mean diameter ($\sim 7.2\ \mu$) and volume (7.4×10^{-11} cm^3) were somewhat smaller than those of the parent red cells.

Figure 3.4:4 shows the tumbling of an 11- and a 16-cell rouleau of red cells in Poiseuille flow at a shear rate $\dot{\gamma} < 10\ \text{sec}^{-1}$ (at shear stress < 0.2 dyn cm^{-2}). This was observed at very low Reynolds numbers, and in a very dilute suspension.

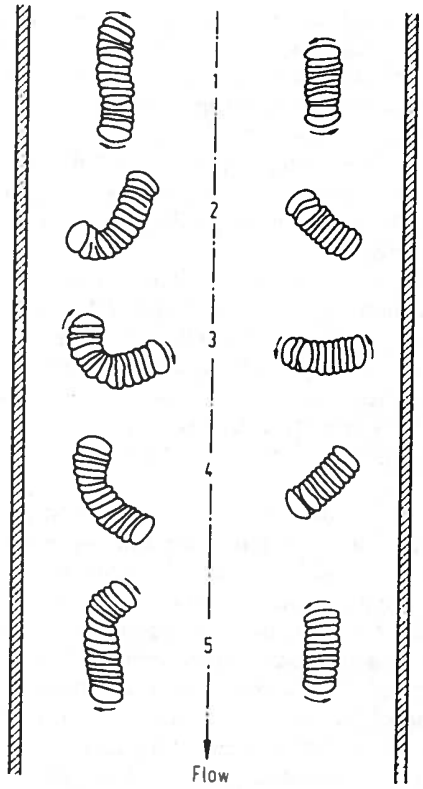

Figure 3.4:4 Rotation of an 11- and a 16-cell rouleau of erythrocytes in Poiseuille flow; $\dot{\gamma} < 10\ \text{sec}^{-1}$. Bending commenced at position 2 where the fluid stresses are compressive to the rouleaux. The longer particle did not straighten out in the succeeding quadrant, in which the stresses in the rouleaux are tensile. From Goldsmith and Marlow (1972), by permission.

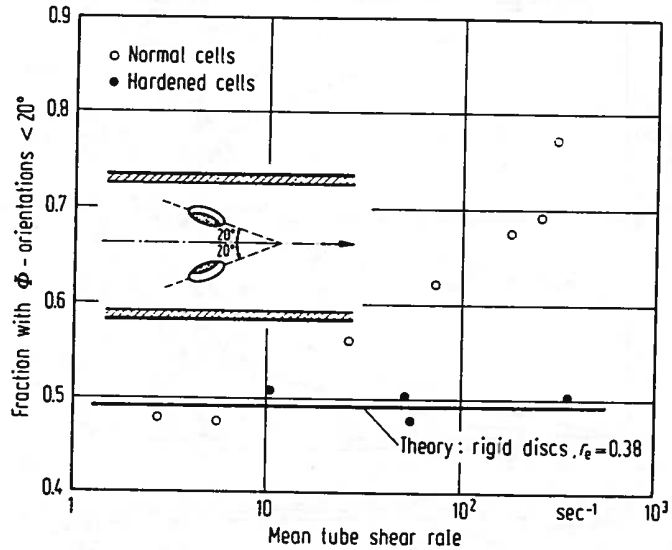

Figure 3.4:5 The increasing fraction of normal red cells (open circles) found in orientation within $\pm 20^\circ$ with respect to the direction of flow as the shear rate is increased in a tube flow. The orientation distribution of hardened cells (closed circles) is independent of the flow speed and radial location in the tube, and agrees with that calculated for rigid disks having an equivalent thickness-to-diameter ratio of $r_e = 0.38$. From Goldsmith (1971), by permission.

The tendency of the deformable red cells to be aligned with the streamlines of flow at higher shear rates is illustrated in Fig. 3.4:5 which refers to observations made in very dilute suspensions in which particle interactions were negligible. It is seen that as the shear rate $\dot{\gamma}$ was increased, more and more cells were found in orientations in which their major axes were aligned with the flow. By contrast, rigid but still biconcave erythrocytes, produced by hardening with gluturaldehyde, continued to show orientations independent of shear rate.

The features shown in Figs. 3.4:4 and 3.4:5 are for isolated red cells or aggregates. Normal blood contains a high concentration of red blood cells,—with a hematocrit ratio (defined as cell volume/blood volume) of about 0.45 in large vessels, and 0.25 in small arterioles or venules. At such a high concentration, the cells crowd each other: no one cell can act alone. Goldsmith's (1972b) observations then show that

(1) The velocity profile in the tube is no longer parabolic as in Poiseuille flow;
(2) deformation of the erythrocytes in blood occurs to a degree that is not attributable to shear alone;
(3) the particle paths exhibit erratic displacements in a direction normal to the flow.

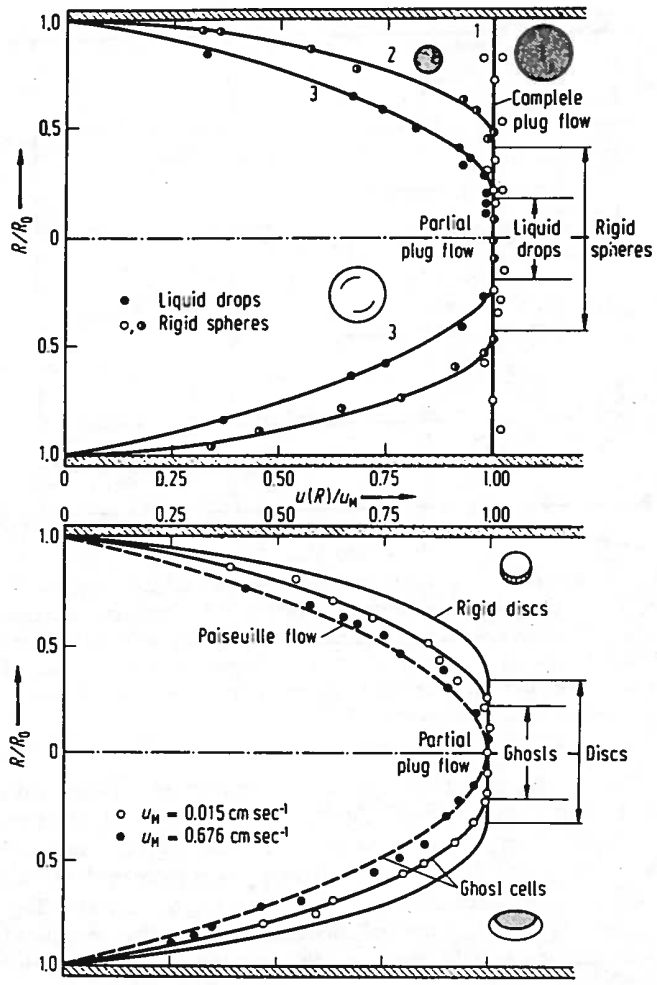

Figure 3.4:6 Comparison of dimensionless velocity profiles of tube flow of a fluid containing particles. b is the radius of the particles. R_0 is the inner radius of the tube. The upper panel shows the flow with 32% suspensions of rigid spheres ($b/R_0 = 0.112$ and 0.056 in curves 1 and 2, respectively) and liquid drops ($b/R_0 = 0.078$, curve 3). The lower panel shows the flow with 32% suspensions of rigid disks ($b/R_0 = 0.078$) and ghost cells ($b/R_0 = 0.105$). The lines drawn are the best fit of the experimental points; the dashed line is calculated from Eq. (6) of Sec. 3.3 in the form $U(R)/U(0) = 1 - R^2/R_0^2$. Note that by complete plug flow in curve 1 (upper part), we do not imply slip of fluid at the wall. Close to the boundary there must be a steep velocity gradient in the suspending fluid. From Goldsmith (1972b), by permission.

The velocity profiles measured in model systems with ghost cells, as well as rigid disks, liquid droplets, and rigid spheres, are shown in Fig. 3.4:6, and can be explained as follows. In a flow of a homogeneous fluid, the profile is parabolic (Poiseuille flow, shown by a dotted line in the lower panel). If there is a *single* isolated *rigid* sphere in the flow, and if the radius of the sphere b is much smaller than the radius of the tube R_0, and if the Reynolds number of the flow is smaller than 1, then the spherical particle will translate along a path parallel to the tube axis with a velocity which, except when the particle is very close to the wall, is equal to the velocity of the undisturbed fluid at the same radial distance. As the concentration of rigid spheres is increased, the particle velocity profile remains parabolic, provided that $b/R_0 < 0.04$ and the volume concentration $c < 0.2$. As the concentration c and the particle-tube-radius ratio b/R_0 are increased further, the velocity profile becomes blunted in the center of the tube. Flow in this central region may be called a *partial plug flow*. For a suspension of rigid spheres the velocity profile is independent of flow rate and suspending phase viscosity, and the pressure drop per unit length of the tube is directly proportional to the volume flow rate $\dot{Q}$. In contrast, flow of a concentrated, monodispersed oil-in-oil emulsion has a velocity profile which is appreciably less blunted than the rigid particle case, at the same values of c and b/R_0, and moreover, this profile is *dependent* on the flow rate and the suspending phase viscosity. In a given system, the lower the flow rate, and the greater the suspending phase viscosity, the greater was the degree of blunting.

Similar non-Newtonian behavior was exhibited by ghost cell plasma suspensions at concentrations from 20% to 70%. Figure 3.4:6 (lower panel) shows the results obtained at a concentration $c = 0.32$, a mean velocity of flow = 1.04 tube diameters per sec; ($U_M = 0.015$ cm sec^{-1}); and a tube radius of 36 μm. Upon increasing the mean velocity of flow to 47 tube diameters per sec ($U_M = 0.676$ cm sec^{-1}), the velocity distribution in the ghost cell suspension became almost parabolic. These features are consistent with the analytical results of Sec. 3.3.

The influence of particle crowding on cell deformation can be expected; but it becomes quite dramatic if we think of the meaning of the curves shown in Fig. 3.4:3. As seen in that figure, the relative viscosity of human blood is considerably lower than that of concentrated oil-in-water emulsions. Are the red blood cells more deformable than the liquid droplets? Are the red cells, in a crowded situation, able to squeeze and move past each other more readily than colliding liquid droplets? The answer is "yes." Direct observation has shown large distortion of red cells and rouleaux at very low shear rates $\dot{\gamma} < 5$ sec^{-1} or shear stress < 0.07 dyn cm^{-2}. An example is shown in Fig. 3.4:7, at a cell concentration (hematocrit) $c = 0.5$. The explanation is believed to lie in the biconcave shape of the red cells. In Chapter 4, Secs. 4.3 and 4.4, it is shown that because of the biconcave shape, the internal pressure of an isolated red cell must be the same as the external pressure if the bending rigidity of the cell membrane is negligibly small. Therefore, the cell membrane

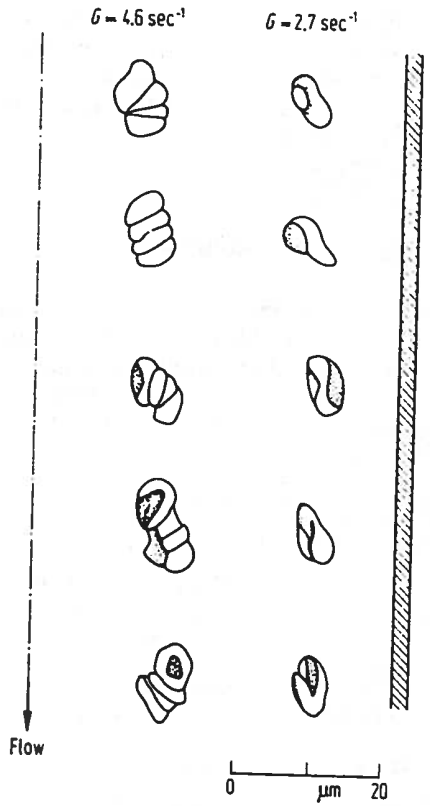

Figure 3.4:7 Tracings from a cine film showing the continuous and irregular deformation of a single erythrocyte and a 4-cell rouleau in a ghost cell suspension, $H = 0.5$. The cell is shown at intervals of 0.4, 0.6, 2.0, and 3.2 s, respectively, in which time the isolated corpuscle would execute just over half a rotation. From Goldsmith (1972a), by permission.

is unstressed in the normal biconcave configuration. Futher, large deformation of the cell can take place without stretching the cell membrane, and hence needs little energy. On the other hand, a liquid droplet in emulsion is maintained by surface tension. In a static condition, a droplet must be spherical if the surface tension is uniform. In a shear flow, the droplets become ellipsoidal in shape; whereas in the crowded situation of a concentrated emulsion, large distortion of shape from that of a regular ellipsoid was noted. Such distortion from the spherical shape increases the surface area of the droplet, and hence the surface energy (surface tension is equal to surface energy per unit area). Thus it becomes plausible that the red cell, by packaging into the biconcave shape, is more deformable than a liquid droplet without a cell membrane. It

also follows from this discussion that a detailed analysis of the rheology of blood or emulsion at high concentration needs data on the viscosities of the liquids and hemoglobin, as well as on the surface tension and cell membrane elasticity.

The third feature of concentrated particulate flow named above; the erratic sidewise movement of particles, has been recorded extensively by Goldsmith. Such erratic motion is expected because of frequent encounters of a particle with neighboring particles. The particle path therefore, must show features of a random walk. These observations offer a qualitative explanation of the way blood flows the way it does.

3.5 Fluid–Mechanical Interaction of Red Blood Cells with a Solid Wall

It has been pointed out by Thoma (1927) that in a tube flow there seems to be a tendency for the red cells to move toward the axis of the tube, leaving a marginal zone of plasma, whose width increases with increase in the shear rate. There is a layer close to the wall of a vessel that is relatively deficient of suspended material. In dilute suspensions, this "wall effect" has been measured by Goldsmith in the creeping flow regime (Reynolds number $\ll 1$). In emulsions the deformation of a liquid drop results in its migration across the streamlines away from the tube wall. Such lateral movement is not observed with rigid spherical particles; thus the deformability of the particle appears to be the reason for lateral migration.

A similar difference in flow behavior was found between normal red blood cells (RBC) and glutaraldehyde-hardened red cells (HBC), as illustrated in the upper panels of Fig. 3.5:1, which show the histograms of the number–concentration distributions of cells as a function of radial distance, at a section 1 cm downstream from the entry in a tube of 83 μm diameter at a Reynolds number about 0.03. Even more striking is the lateral migration in dextran solutions at Reynolds numbers $R_n = 3.7 \times 10^{-3}$ and 9.1×10^{-4}, shown in the lower panels. It is seen that very few cells are present in the outer half of the tube. Dextran solutions have a higher viscosity than Ringer or Ringer-plasma solutions. In dextran solutions the red cells are deformed into ellipsoidlike shapes. Similar observations of flow containing rouleaux of red cells show that rouleaux migrate to the tube axis faster than individual red cells.

Inward migration of deformable drops, fibers, and red cells away from the wall in both steady and oscillatory flows has been observed also at higher Reynolds numbers ($R_n > 1$), when the effects of fluid inertia are significant. At $R_n > 1$ nondeformable particles also exhibit lateral migration in dilute suspensions.

When the cell concentration is high, the crowding effect acts against migration away from the wall into the crowded center. Measurements made by Phibbs (1969) in quick-frozen rabbit femoral arteries, by Bugliarello and

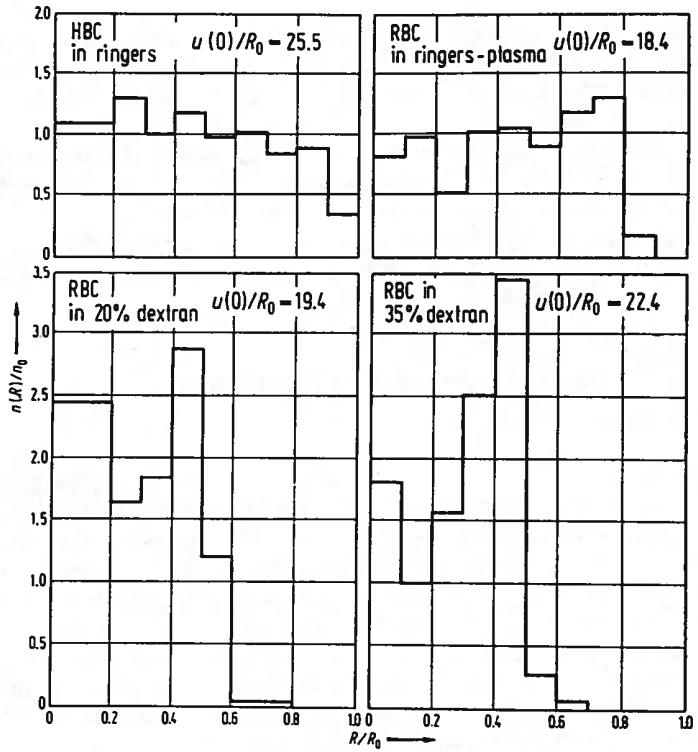

Figure 3.5:1 Number of cells/cm^3 suspension, $n(R)$, divided by the syringe reservoir concentration, n_0, at intervals of 0.1 R_0, 1 cm downstream from the reservoir; R_0 = 41.5 μm, $c = 2 \times 10^{-3}$. The mean tube shear rates = $u(0)/R_0$ were approximately the same in each suspension. If the number distribution were uniform, then $n(R)/n_0 = 1$ at all R/R_0. From Goldsmith (1972b), by permission.

Sevilla (1971) on cine films of blood flow in glass tube, and by Blackshear et al. (1971) on ghost cell concentration, make it appear unlikely that at hematocrits of 40%–45% and normal flow rates, the plasma-rich zone can be much larger than 4 μm in vessels whose diameters exceed 100 μm.

This plasma-rich (or cell-rare) zone next to the solid wall, although very thin, has important effect on blood rheology. In the first place, measurement of blood viscosity by any instrument which has a solid wall must be affected by the wall layer. The change in cell concentration in the wall layer makes the blood viscosity data somewhat uncertain. Thus we are forced to speak of "apparent" viscosity (see Chapter 5, Sec. 5.1), rather than simply of the viscosity. It makes it necessary to specify how "smooth" or "serrated" the surface of viscometers must be. In the second place, the smaller the blood vessel is, the greater will be the proportion of area of the vessel occupied by the wall

layer, and greater would be its influence on the flow. The low hematocrit in the wall layer lowers the average hematocrit in small blood vessels. And when a small blood vessel branches off from another vessel, it draws more fluid from the wall layer where the hematocrit is low. The result is a lower average hematocrit in the smaller blood vessel; and hence a lower apparent viscosity. This will be discussed in Chapter 5.

3.6 Thrombus Formation and Dissolution

Blood clots are formed on an injured inner wall of blood vessels and on contact with the surfaces of medical devices. When a circulating blood comes into contact with such a surface, the platelets in the blood adhere to the surface, release a number of chemicals, attract more platelets to form a larger aggregation, generate thrombin, and form fibrin, resulting in a thrombus. In time

TABLE 3.6:1 Properties of Human Clotting Factors*

Clotting factor	Synonym	Molecular weight (number of chains)	Normal plasma concentration (μg/ml)
Intrinsic system			
Factor XII	Hageman or contact factor	80 000 (1)	29
Prekallikrein	Fletcher factor	80 000 (1)	50
High-molecular-weight Kininogen	Fitzgerald factor	120 000 (1)	70
Factor XI	Plasma thrombo-plastin antecedent	160 000 (2 dimer)	4
Factor IX	Christmas factor	57 000 (1)	4
von Willebrand factor	vWF	1–2 000 000 (series of G-10 subunits)	7
Factor VIII:C	Antihemophilic factor	200 000–350	0.1
Extrinsic system			
Factor VII	Proconvertin	55 000 (1)	1
Tissue factor	Tissue thromboplastin	45 000 (1)	1
Common pathway			
Factor X	Stuart–Prower factor	59 000 (2)	5
Factor V	Proaccelerin	330 000 (1)	5–12
Prothrombin	Factor II	70 000 (1)	100
Fibrinogen	Factor I	340 000 (6: $A\alpha_2, B\beta_2, \gamma_2$)	2500 (250 mg/dl)
Factor XIII	Fibrin stabilizing factor	300 000 (4: a_2, b_2)	10

*Factor III is tissue thromboplastin. Factor IV is calcium. There is no factor VI.

plasmin is generated in the thrombus, and fibrinolysis begins, ending in the dissolution of the thrombus.

The blood clotting process is a cascade of chemical processes with many participants. The principal chemicals are listed in Table 3.6:1. In the table, those activating and coagulation factors reside in the blood plasma are called *intrinsic*, those residing in the cells (not in the plasma) are called *extrinsic*. A very brief sketch is given below. Details should be obtained from hematological, pharmacological, and medical books. An National Institute of Health (NIH) report edited by McIntire (1985) is very helpful.

3.6.1 Thrombogenesis

Figure 3.6:1 shows the major chemicals involved at the first stages of platelet adhesion and aggregation. The injured endothelium exposes collagen of the basement membrane which interacts with the glycoprotein on the platelet membrane and the von Willebrand factor which is synthesized by endothelial cells and is present in the plasma, and on the platelets. The adherent platelets then release adenosine diphosphate (ADP), thromboxane A_2, fibrinogen, factor *V*, platelet factor 4, beta thromboglobulin, and a platelet-derived growth factor.

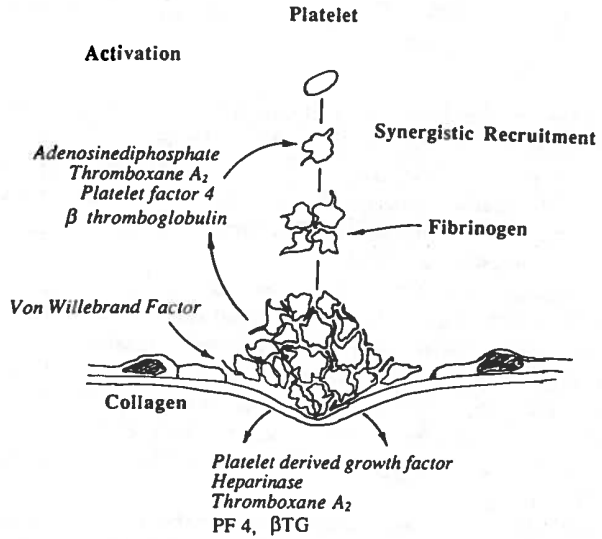

Figure 3.6:1 Platelet adhesion and aggregation after an injury of the blood vessel wall. Aggregation of platelets requires a rapid mobilization of fibrinogen receptors on the membranes of the platelets, and a calcium-dependent interplatelet bridging by fibrinogen. Various factors are shown. Figure was redrawn after an example in *Guidelines for Blood–Material Interactions*, which is a Report of the National Heart, Lung, and Blood Institute (NHLBI) Working Group of the U.S. Department of Health and Human Services, Public Health Service NIH Publ. No. 85–2185, 1985.

The released ADP and thromboxane A_2 act synergistically to recruit circulating platelets and enlarge the aggregate. Essential to this step is the mobilization of a platelet-membrane fibrinogen receptor and the calcium-dependent interplatelet bridging by fibrinogen.

Thrombus growth and stabilization depends on the formation of thrombin. Thrombin is generated by means of the intrinsic coagulation pathway through contact factor activation by subendothelial collagen, or when tissue thromboplastin from disrupted endothelial cells activates the extrinsic coagulation cascade. Once formed, thrombin stimulates the synthesis of thromboxane A_2 and the release of ADP, thus promoting platelet aggregation. Subsequently, thrombin generates fibrin from fibrinogen. Fibrin stabilizes the growing platelet mass to form a viscoelastic clot.

The contact factor (Hageman, or factor XII) activation begins by the adsorption of the contact factor to the negatively charged collagen surface. Factors XI, prekallikrein, and kininogen are also involved. This step is calcium independent. The adsorption of factor XII to collagen changes the molecular configuration of factor XII and exposes its hydrophobic active sites previously unavailable to the external environment, and the intrinsic system cascade begins. The fibrinolytic system is also activated by factor XII via plasminogen proactivator. Factors XI, V, and the von Willebrand factor may also be adsorbed to an artificial surface.

The activation of factor IX by XIa and the activation of factor X are calcium dependent. Factors IX, X, VII, and prothrombin are vitamin K dependent.

The *extrinsic system* is initiated by the activation of factor VII when it interacts with an intracellular tissue factor, or leukocytes. Tissue factor is present in large amounts in the brain and lung, and found in the intima of large blood vessels.

The *common pathway* begins as factor X is activated by factor VIIa or IXa.

The concentration of prothrombin in plasma is sufficient to allow a few molecules of activated initiator to generate a large burst of thrombin activity, which induces platelet aggregation, and converts fibrinogen into fibrin. Fibrin monomers polymerize nonenzymatically to gelate the fluid.

3.6.2 Thrombus Dissolution

Within the thrombus, plasmin digests fibrin to produce progressively smaller fragments to eventually dissolve the clot. The blood contains plasminogen (molecular weight 90 000, normally at the 120 μg/ml level) which is enmeshed in the thrombus. It can be activated intrinsically by the contact factor XII, etc.; or extrinsically with an activator originating from the blood vessel wall; or by drugs such as streptokinase or urokinase. Activation releases plasmin. Plasmin is an active serine protease, which hydrolyzes fibrin polymers.

TABLE 3.6:2 Antithrombotic Agents

Agent	Action
Fibrinolytic	
Streptokinase, urokinase	Plasminogen activators
Anticoagulant	
Heparin	Enhances inhibition of proteases by thrombin III
Warfarin	Vitamin K antagonist
Antiplatelet	
Aspirin	Decreases platelet aggregation and release
Sulfinpyrazone	Not established
Dipyridamole	Decreases platelet adhesion
Ticlopidine	Blocks ADP induced platelet interaction with fibrinogen and vWF
PGI_2	Activates platelet adenyl cyclase

In practice, a thrombus can be continuously formed and dissolved; so its composition is a result of chemical dynamics. Some well-known antithrombotic agents are listed in Table 3.6:2.

Thrombosis can be a threat to life. But it can stop internal bleeding if there were a break in the blood vessel, or external bleeding when there is an injury. Coagulation of blood seals the wound and saves lives. Contraction of the damaged blood vessels is another mechanism of life saving.

Blood coagulation is the result of a cascading activation of factors. An almost total absence of any one of these factors will make the coagulation process extremely slow. For example, if one takes the calcium away, blood will not clot. If one draws blood with a collecting vessel treated with oxalate or citrate, the blood will flow freely. Rheological studies of blood clotting are often made either for clinical reasons or for pharmacological development. A summary of some more popular instruments is given in Scott-Blair (1974). The instrument 'thrombelastograph" of Hartert (1962, 1975) needs blood sample of only 0.3 ml.

3.7 Medical Applications of Blood Rheology

The most obvious use of blood rheology in clinical medicine is to identify diseases with any change in blood viscosity. Data collected for this purpose have been presented by Dintenfass in two books (1971, 1976). For our purpose it suffices to cite a few examples. Figure 3.7:1 shows a comparison of

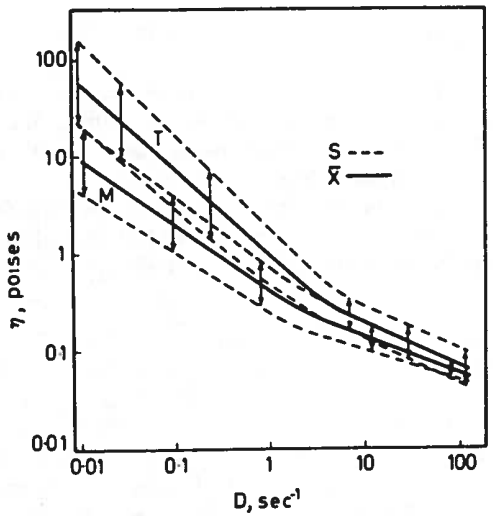

Figure 3.7:1 Arithmetic means (full lines) and one standard deviation (broken lines) of viscosities in normal men (M) and in patients with various thrombotic diseases (T). Viscosity, η, in poises, is plotted against the rate of shear, D, in sec^{-1}, on a log–log scale, where $\bar{x}$ is the arithmetic mean, and s is the standard deviation. Experimental data show log-normal distribution. From Dintenfass (1971), p. 11, by permission.

Dintenfass' data on the blood viscosity of normal healthy persons and patients with various thrombotic diseases. The diseased persons have higher viscosity. As we have seen in Sec. 3.4, elevation of blood viscosity at low shear rates indicates aggregation, whereas that at high shear rates suggests loss of deformability of the red blood cells. The viscosity change suggests some disease related changes in the blood.

Figure 3.7:2 suggests another use of lowered blood viscosity. It shows Langsjoen's (1973) result that a reduction of blood viscosity consequent to the infusion of dextran 40 solution in cases of acute myocardial infarction led to a significant improvement in both immediate and long-term survival. Dextran 40 (molecular weight about 40 000) solution dilutes the blood. The physiological effect of hemodilution is not simple, but the changed rheology must be a principal factor. For hemodilution, see Messmer and Schmid-Schoenbein (1972).

The fluid added to the bloodstream to make up the lost volume of blood due to hemorhage when a person suffers a wound is called *plasma expander*. Dextran solution is a good expander. Any blood substitute for long term use must have the right rheological property.

Another important rheological factor in clinical use is the coagulation characteristics of the blood. An obvious example is the hemophilic patient's difficulty with blood coagulation. On the other hand, hypertension (high

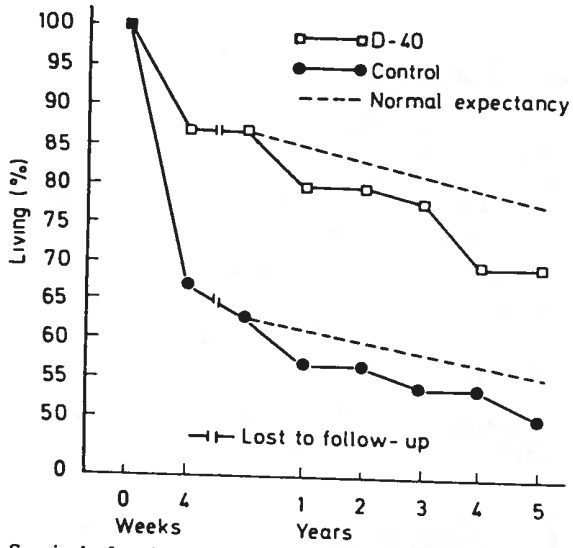

Figure 3.7:2 Survival of patients with acute myocardial infarction after conservative treatment (73 patients) and after treatment by infusion of dextran 40 (65 patients). Survival is recorded as the percentage of the original group. Note that there were more surviving patients in the dextran-treated group after 5 years than in the controls (conservative treatment) after 4 weeks. This gives cogent support to the premise that blood viscoscity is an important determinant of myocardial work. Reproduced from Langsjoen (1973), by permission.

blood pressure) and arteriosclerosis seem to correlate with an increase in the elasticity of the thrombi.

A third parameter in clinical use is the *erythrocyte sedimentation rate*. In anticoagulated blood, red cells may still clump together and cause a sedimentation. Fahraeus (1918) first studied this effect seriously. He noticed that blood from pregnant women sedimented faster than that of nonpregnant women, and believed that he might have found a convenient test for pregnancy. However, he soon afterwards found the same more rapid sedimentation in some male patients! It was then established that an increased erythrocyte sedimentation rate served as a good indication for both male and female patients that all was not well, and that quite a variety of conditions, many of them serious, increased the sedimentation rate. This is discussed in considerable detail in Dintenfass (1976).

It is quite clear that blood rheology as discussed in this chapter, referring to flow in vessels much larger than the diameter of red blood cells, reflects the interaction of red cells in bulk of whole blood. The "hyperviscosity" of blood in some disease states reflects the changes in hematocrit, plasma, and red cell deformability. On the other hand, the critical sites of interaction of red blood cells with blood vessels are in the capillary blood vessels. In the

microcirculation bed, the deformability of the red cells is subjected to a really severe test. Hence it is expected that the pathological aspects of hyperviscosity will be seen in microcirculation. To pursue this matter, we shall consider the mechanical properties of red cells in the following chapter, and the flow properties of blood in microvessels in Chapter 5.

Problems

3.1 Show that, for an incompressible fluid, $I_1 = 0$, where I_1 is given in Eq. (3) of Sec. 3.2.

3.2 Thus far we have treated blood as a viscous fluid. This is undoubtedly permissible if blood flows in a steady-state condition. But since blood is a suspension of blood cells in plasma, and the cells are capable of interacting with each other, it is expected that blood will exhibit viscoelastic properties when conditions permit, just like many other polymer solutions. Speculate, on theoretical grounds, on what may be expected in the following situations:

(a) A volume of blood sits in a condition of stationary equilibrium in a Couette viscometer or in a circular cylindrical tube (Poiseuille viscometer). A harmonic oscillation of very small amplitude is imposed on the blood in the viscometer. What would be the relationship between force and velocity? How would one express the relationship through the method of a complex variable? What is the phase relationship? What do the real and imaginary parts of the complex modulus mean?

(b) Let the blood in the viscometer flow in a steady state and then superimpose a small harmonic oscillation on the flow in the viscometer. How would the complex modulus vary with the steady-state shear strain rate?

(c) Instead of harmonic oscillations of small amplitude as considered above, impose a small step function in velocity (Couette) or pressure gradient (Poiseuille), and discuss the expected response as a function of time.

(d) If the step function considered in (c) is finite in amplitude, could there be nonlinear effects which depend on the amplitude? The change in viscoelastic properties of a material with respect to time after a finite disturbance is called a *thixotropic* change. Thixotropy of blood may be described by a complex modulus of viscosity as a function of time after the initiation of disturbance (e.g., a step function); the modulus being obtained by a superposed small harmonic perturbation. Speculate on the possible thixotropic properties of blood.

Experimental results on the features named above as well as a mechanical and mathematical model of the viscoelasticity of blood expressed in terms of springs and dashpots are discussed by G. B. Thurston (1979).

3.3 *Entry flow of blood from a large reservoir into a pipe.* So far we have analyzed the condition of flow in a pipe in a region far away from the entry section. At the entry section ($x = 0$), where the pipe is connected to a large reservoir, the velocity profile is uniform, as shown in Fig. 3.3:1. As the distance from the entry section increases, the profile changes gradually to the steady-state profile of a parabola (if the fluid is Newtonian) or the flat-topped parabola of Fig. 3.3:4 (if the fluid is blood). Consider blood. We can trace the change as sketched in Fig. P3.3. At

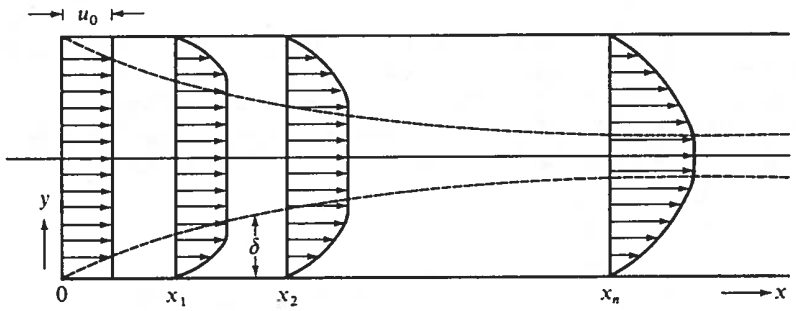

Figure P3.3 Entry flow of blood into a pipe. Dotted lines show the boundary layer of yielding.

$x = x_1$ the velocity has to change from u_0 at the center to 0 on the wall, where the no-slip condition applies. This creates a high shear strain rate at the wall, which has to decrease to zero at the center. At a certain distance δ from the wall is a point where the shear stress is equal to the yield stress of the blood. Beyond $y = \delta$, the velocity profile remains flat. As x increases, δ increases. At $x = x_n$ the velocity profile tends to the steady state, as shown in Fig. 3.3:4.

The surface $y = \delta(x)$ is the *yielding surface*, which divides the region (at the center) in which the blood is solid-like, from the region (next to the wall) in which the blood is a flowing fluid. It is a surface on which the shear stress is exactly equal to the yield stress. The rate at which $\delta(x)$ grows with x depends on the Reynolds number of flow N_R. Give a qualitative and mathematical analysis of $\delta(x)$ as a function of N_R.

3.4 With the constitutive equations of blood presented in Sec. 3.2, derive the equation of motion of blood in a form that is a generalization of the Navier–Stokes equation. Discuss the range of validity of the equations. Discuss any simplification that results if the shear strain rate is sufficiently high.

3.5 *Boundary Conditions.* The general field equations of continuity and motion are to be solved with boundary conditions which must be posed in such a way that the field equations have meaningful solutions, and must lead to solutions in agreement with experimental results. The condition at the interface between a fluid and a solid has raised the question of whether to allow relative slip between fluid and solid or not. Historically, for water, the question was resolved in favor of *no-slip* on the basis of precise experimental results of Poiseuille and Hagen on flow in circular cylindrical tubes. For Newtonian fluids the *no-slip* condition between fluid and solid has been established and has found no exception in the past 150 years.

Blood is a mixture of cells and a fluid. Consider the conditions at a blood–solid interface theoretically. What should the boundary conditions be?

3.6 Reduce the equations you obtained in Problem 3.4 to a dimensionless form. Introduce a characteristic length L, a characteristic velocity V, a characteristic viscosity η which is one of the constants in Eq. (12b) of Sec. 3.2, and dimensionless coordinates $x_i' = x_i/L$, velocities $u_i' = u_i/V$, and parameters

$$p' = \frac{p}{\rho V^2}, \qquad t' = \frac{Vt}{L}, \qquad N_R = \frac{VL\rho}{\eta},$$

where N_R is the Reynolds number.

3.7 If laboratory model testing is to be done for blood flow, on what basis would you design the models. A scaled model may be desired to facilitate observations on velocity, pressure, forces, etc. It may be convenient to use water or a polymer fluid as the working fluid in place of blood plasma. Discuss the principles of kinematic and dynamic similarities in model design.

3.8 Assume that Casson's equation [Eq. (11) of Sec. 3.2] describes the viscosity of blood. Both τ_y and η are functions of the hematocrit. Experimental data (see Fig. 3.1:5) on τ_y may be presented by an empirical formula,

$$\tau_y = (a_1 + a_2 H)^3.$$

For normal blood, we may take $a_1 = 0$, $a_2 = 0.625$, when τ_y is in dyn cm^{-2} and H, the hematocrit, is a fraction. Experimental data on η can be expressed in many ways. Let us assume that for large blood vessels (Cokelet et al., 1963)

$$\eta = \eta_0 \frac{1}{(1 - H)^{2.5}},$$

where η_0 is the viscosity of the plasma.

For the capillary blood vessels Casson's equation does not hold: but we may assume

$$\mu = \eta_0 \frac{1}{1 - CH}.$$

We may take an average value $C = 1.16$ for pulmonary capillaries (Yen-Fung, 1973) and H in capillaries to be 0.45 times that of the systemic hematocrit in large arteries. The peripheral resistance from capillary blood vessels may be assumed to be a constant fraction of the total peripheral resistance. For the lung this fraction may be as high as $\frac{1}{3}$. For other parts of the body, this fraction is perhaps 15%.

With these pieces of information, let us consider the question "What is the best hematocrit that minimizes the work of the heart while the total amount of oxygen delivered to the tissues of the body remains constant?" Such a question is important in surgery or hemodilution, in deciding the proper amount of plasma expander to use.

To answer this question we may consider blood flow as a flow in large and small vessels in series. The pressure drop in each segment is equal to the flow times the resistance which is proportional to blood viscosity. The total pressure difference the heart has to create is the sum of the pressure drop of the segments. The rate at which work is done by the heart is equal to the cardiac output (flow) times the pressure difference. The total amount of oxygen delivered to the tissues is proportional to the product of cardiac output and the hematocrit if the lung functions normally.

What would be the optimum hematocrit if the blood pressure is fixed and oxygen delivery is maximized?

3.9 The analysis of tube flow given in Sec. 3.3 ignores the radial migration of red cells away from the wall. As discussed in Sec. 3.5, for blood flowing in a tube, the immediate neighborhood of the solid wall is cell free. For human blood with a red

cell concentration above 0.4 and tube diameter > 100 μm, the cell-free layer is a about 4 μm thick. For a dilute suspension, e.g., at red cell concentration 0.03, the thickness of the cell-free layer is larger (see Fig. 3.5:1). Use the information on the dependence of the constants τ_y and η of the Casson equation on the hematocrit as given in Problem 3.8 to revise the velocity profile and flow rate given in Eqs. (19) and (21) of Sec. 3.3. For this purpose assume the hematocrit to be constant away from the cell-free layer next to the wall. This assumption is quote good at normal hematocrit (0.2–0.5), but is rather poor for very dilute suspensions.

3.10 Consider the effect of non-Newtonian features of blood on the Couette flow of blood between concentric circular cylinders. Assume the outer cylinder to rotate, the inner cylinder stationary, Casson's equation to apply, cell-free layers next to solid walls with a thickness of a few (say, 4) μm, and absence of end effects.

3.11 Analyze blood flow in a cone-plate or a cone–cone viscometer analogous to Problem 3.10.

3.12 Blood exposed to air will form a surface layer at the interface, which has a specific surface viscosity and surface elasticity, depending on the plasma constitution. In viscometry using a Couette-flow or cone-plate arrangement, one must avoid reading the torque due to the surface layer. A *guard ring* was invented to shield the stationary cylinder from the torque transmitted through the surface layer. The ring can be held in place by an arm that is fixed to the laboratory floor, and unattached to the instrument. Propose a design for such a guard ring.

3.13 Consider the following thought experiment. Take normal red blood cells and suspend them in an isotonic dextran solution of viscosity η_0. η_0 can be varied by varying the concentration of dextran. Measure the viscosity at a sufficiently high shear rate $\dot{\gamma}$ so that the influence of cell aggregates is insignificant. Let the viscosity be $\mu = \eta_r \eta_0$, where η_r is the "relative viscosity." How would η_r vary with η_0? η_r reflects the effect of cell deformation. Would the red cells be more readily deformed in a more viscous suspending medium? Or less so? Predict curves of η_r vs. $\dot{\gamma}$ for various values of η_0.

Note. The effect of cell deformation on the apparent viscosity depends on the flow condition. Consider Couette flow which is a case investigated by Chien (1972) experimentally. In this case η_r decreases monotonically when the shear strain rate increases.

3.14 Discuss the pros and cons for several types of viscometers from the point of view of practical laboratory applications (convenience of operation, accuracy of data, amount of fluid samples needed, data reduction procedures, and procedures required for correction of errors).

3.15 Consider the flow of a Newtonian viscous fluid in a straight tube of infinite length and a rectangular cross section of width a and thickness b. Derive the equation that governs the velocity distribution in the tube. Express the volume flow rate as a function of the pressure gradient and the dimensions of the cross section. Obtain results for the specially simple case in which $b \gg a$. Then repeat the analysis if the fluid obeys Casson's equation, at least for the case in which $b \gg a$.

3.16 A fluid is said to obey a *power law* viscosity if the shear stress τ in a Couette flow is related to the shear rate $\dot{\gamma}$ by the equation

$$\dot{\gamma} = \frac{1}{k}\tau^n \qquad (n > 0). \tag{1}$$

This relationship is illustrated in Fig. P3.16.

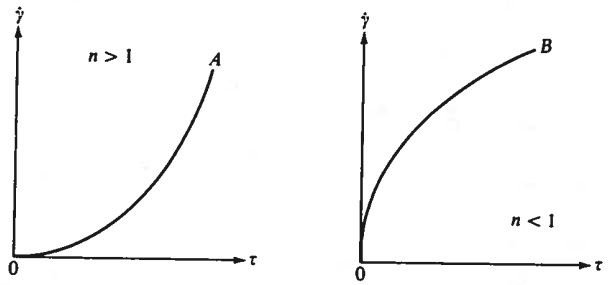

Figure P3.16 Power-law viscosity. Curve A, $n > 1$; curve B, $n < 1$.

For a steady flow of an incompressible fluid obeying the power law (1) in a circular cylindrical tube of radius R, show that the axial velocity is

$$u = \frac{1}{2^n(n+1)k}\left(\frac{\Delta p}{L}\right)^n (R^{n+1} - r^{n+1}), \tag{2}$$

where Δp is the difference of pressures at the ends of a tube of length L. The rate of flow (volume) is

$$Q = \frac{\pi R^{n+3}}{2^n(n+3)k}\left(\frac{\Delta p}{L}\right)^n. \tag{3}$$

Let the average velocity be $U = Q/\pi R^2$, then

$$\frac{u}{U} = \frac{n+3}{n+1}\left[1 - \left(\frac{r}{R}\right)^{n+1}\right]. \tag{4}$$

3.17 A material is said to be a *Bingham plastic* if the shear stress τ is related to the shear rate $\dot{\gamma}$ by the equation

$$\dot{\gamma} = \frac{1}{\eta_B}(\tau - f_B) \quad \text{when} \quad \tau > f_B; \qquad \text{and} \qquad \dot{\gamma} = 0 \quad \text{when} \quad \tau < f_B.$$

The stress f_B is called the *yield stress*. The constant η_B is called *Bingham viscosity*. The relation is illustrated in Fig. P3.17.

The steady flow of a Bingham plastic in a circular cylindrical tube of length L subjected to a pressure difference Δp can be analyzed in a manner similar to that presented in Sec. 3.3. Show that:

(a) If $\dfrac{\Delta p}{L} > \dfrac{2f_B}{R}$ and $r_B = \dfrac{2f_B L}{\Delta p}$, then

$$u = \frac{\Delta p}{4\eta_B L}(R - r_B)^2 \qquad \text{when} \quad r < r_B,$$

$$= \frac{\Delta p}{4\eta_B L}[R^2 - r^2 - 2r_B(R - r)] \qquad \text{when} \quad r > r_B.$$

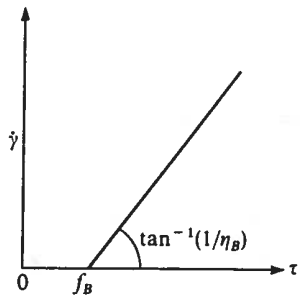

Figure P3.17 Flow curve of a Bingham plastic.

(b) If $\frac{\Delta p}{L} < \frac{2f_B}{R}$, then there is no flow: $u = 0$.

The flow rate is zero if $\Delta p < p_B \equiv 2Lf_B/R$, and is

$$Q = \frac{\pi R^4}{8\eta_B L}\left[\Delta p - \frac{4}{3}p_B + \frac{1}{3}\frac{p_B^4}{(\Delta p)^3}\right] \qquad \text{if} \quad \Delta p > p_B.$$

3.18 A plastic material obeying the following relation between the shear stress τ and shear rate $\dot{\gamma}$ is called a plastic of *Herschel–Bulkley* type:

$$\dot{\gamma} = \frac{1}{k}(\tau - f_H)^n \qquad \text{if} \quad \tau > f_H, \qquad \text{and} \qquad \dot{\gamma} = 0 \qquad \text{if} \quad \tau < f_H,$$

where k, f_H, and $n > 0$ are constants. The Bingham plastic of Problem 3.17 is a special case in which $n = 1$, whereas the power law of Problem 3.16 is a special case when $f_H = 0$. For the general case, find the velocity distribution in a steady laminar flow of an incompressible Herschel–Bulkley fluid in a circular cylindrical tube.

3.19 Discuss the turbulent flow of water in a circular cylindrical tube. Consider the question of the relationship of mean velocity of flow with pressure gradient. Does it remain linear? How is the flow rate related to pressure gradient? Discuss resistance to flow in a turbulent regime.

Note. Many books deal with this subject. See references listed in Chapter 11 of Fung, *A First Course in Continuum Mechanics.*

3.20 Prove that blood viscosity as we know it cannot be represented by the Boltzmann equation

$$\tau(t) = \int_{-\infty}^{t} G(t-\tau)\frac{d\gamma(\tau)}{d\tau}d\tau,$$

where $\tau(t)$ is the shear stress, $\gamma(t)$ is the shear strain rate, and $G(t-\tau)$ is a continuous function of the variable $t - \tau$.

3.21 A Newtonian fluid flows steadily through a capillary tube whose radius R is

$$R(x) = a + \varepsilon \sin\frac{\pi x}{L}$$

where a, L, and ε are constants, with $\varepsilon \ll a$, $L \gg a$. The Reynolds number of flow is small, $\ll 1$. What is the pressure distribution in the tube as a function of x?

Hint. Under the assumption that $\varepsilon/a \ll 1, a/L \ll 1$, you may treat the Poiseuille equation as a differential equation for the pressure p:

$$\frac{dp}{dx} = -\frac{8\mu Q}{\pi R^4}$$

Q is constant, R is variable. Solve the equation above as a power series in ε/a.

3.22 Consider an elastic tube whose radius R varies with the pressure according to the following law:

$$R(x) = a(x)[1 + \alpha p(x)],$$

where p is the local transmural pressure, α is the flexibility coefficient, and $a(x)$ is the radius of the tube when $p = 0$. $a(x)$ is a function of x and is not a constant. For a constant blood viscosity μ and a one-dimensional flow in a tube of length L, what is the volumetric flow rate $\dot{Q}$ in the tube as a function of the pressures at the entry (p_a) and exit (p_v) of the tube? α is a constant. Use the hint given in Prob. 3.21.

3.23 Derive the following equations for the laminar steady flow of a non-Newtonian incompressible fluid in a circular cylindrical tube; under the assumption that the shear stress τ_w at the wall is a single-valued function of the local rate of deformation:

$$\tau_w = \frac{D(\Delta p)}{4L},$$

$$\dot{\gamma}_w = \frac{\tau_w}{4}\frac{d}{d\tau_w}\left(\frac{8\bar{V}}{D}\right) + \frac{3}{4}\left(\frac{8\bar{V}}{D}\right),$$

where $\dot{\gamma}_w$ = shear rate at the wall,
D = tube diameter,
ΔP = axial pressure difference for two points at a distance L apart,
L = axial distance,
$\bar{V}$ = bulk average velocity.

Ref. Markovitz, 1968. *Physics Today*, **21**, 23–30.

References

Barbee, J. H. and Cokelet, G. R. (1971) The Fahraeus effect. *Microvasc. Res.* **3**, 1–21.

Biggs, R. and MacFarlane, R. G. (1966) *Human Blood Coagulation and Its Disorders*, 3rd edition. Blackwell, Oxford.

Blackshear, P. L., Forstrom, R. J., Dorman, F. D., and Voss, G. O. (1971) Effect of flow on cells near walls. *Fed. Proc.* **30**, 1600–1609.

Brooks, D. E., Goodwin, J. W., and Seaman, G. V. F. (1970) Interactions among erythrocytes under shear. *J. Appl. Physiol.* **28**, 172–177.

Bugliarello, G. and Sevilla, J. (1971) Velocity distribution and other characteristics of steady and pulsatile blood flow in fine glass tubes. *Biorheology* **7**, 85–107.

Casson, M. (1959) A flow equation for pigment-oil suspensions of the printing ink type. In *Rheology of Disperse Systems*, C. C. Mills (ed.) Pergamon, Oxford, pp. 84–104.

Charm, S. E. and Kurland, G. S. (1974) *Blood Flow and Micro Circulation*. Wiley, New York.

Chien, S. (1970) Shear dependence of effective cell volume as a determinant of blood viscosity. *Science* **168**, 977–979.

Chien, S. (1972) Present state of blood rheology. In *Hemodilution. Theoretical Basis and Clinical Application*, K. Messmer and H. Schmid-Schoenbein (eds.) Int. Symp. Rottach-Ergern, 1971, S. Karger, Basel, pp. 1–45.

Chien, S., Usami, S., Taylor, M., Lundberg, J. L., and Gregersen, M. I. (1966) Effects of hematocrit and plasma proteins of human blood rheology at low shear rates. *J. Appl. Physiol.* **21**, 81–87,

Chien, S., Usami, S., and Dellenbeck, R. J. (1967) Blood viscosity: Influence of erythrocyte deformation. *Science* **157**, 827–831.

Chien, S., Usami, S., Dellenbeck, R. J., and Gregersen, M. (1970) Shear dependent deformation of erythrocytes in rheology of human blood. *Am. J. Physiol.* **219**, 136–142.

Chien, S., Luse, S. A., and Bryant, C. A. (1971) Hemolysis during filtration through micropores: A scanning electron microscopic and hemorheologic correlation. *Microvasc. Res.* **3**, 183–203.

Chien, S., Usami, S., and Skalak, R. (1984) Blood flow in small tubes. In E. M. Renkin, and C. C. Michel (eds.) *Handbook of Physiology, Sec. 2, The Cardiovascular System*, Vol. IV, Part 1. American Physiological Society, Bethesda, MD, pp. 217–249.

Cokelet, G. R. (1972) The rheology of human blood. In *Biomechanics: Its Foundation and Objectives*, Fung, Perrone, and Anliker (eds.) Prentice-Hall, Englewood Cliffs, NJ, pp. 63–103.

Cokelet, G. R., Merrill, E. W., Gilliland, E. R., Shin, H., Britten, A., and Wells, R. E. (1963) The rheology of human blood measurement near and at zero shear rate. *Trans. Soc. Rheol.* **7**, 303–317.

Dintenfass, L. (1971) *Blood Microrheology*. Butterworths, London.

Dintenfass, L. (1976) *Rheology of Blood in Diagnostic and Preventive Medicine*. Butterworths, London.

Fung, Y. C. (1965) *Foundations of Solid Mechanics*. Prentice-Hall, Englewood Cliffs, NJ.

Fung, Y. C. (1993) *A First Course in Continuum Mechanics*, 3rd edition. Prentice-Hall, Englewood Cliffs, NJ.

Goldsmith, H. L. (1971) Deformation of human red cells in tube flow. *Biorheology* **7**, 235–242.

Goldsmith, H. L. (1972a) The flow of model particles and blood cells and its relation to thrombogenesis. In *Progress in Hemostasis and Thrombosis*, Vol. 1, T. H. Spaet (ed.) Grunte & Stratton, New York, pp. 97–139.

Goldsmith, H. L. (1972b) The microrheology of human erythrocyte suspensions. In *Theoretical and Applied Mechanics Proc. 13th IUTAM Congress*, E. Becker and G. K. Mikhailov (eds.) Springer, New York.

Goldsmith, H. L. and Marlow, J. (1972) Flow behavior of erythrocytes. I. Rotation and deformation in dilute suspensions. *Proc. Roy. Soc. London B* **182**, 351–384.

Gregersen, M. I., Bryant, C. A., Hammerle, W. E., Usami, S., and Chien, S. (1967) Flow characteristics of human erythrocytes throughy polycarbonate sieves. *Science* **157**, 825–827.

Hartert, H. and Schaeder, J. A. (1962) The physical and biological constants of thrombelastography. *Biorheology* **1**, 31–40.

Hartert, H. (1975) Clotting layers in the rheo-simulator. *Biorheology* **12**, 249–252.

Haynes, R. H., (1962) The viscosity of erythrocyte suspensions. *Biophys. J.* **2**, 95–103.

Langsjoen, P. H. (1973) The value of reducing blood viscisity in acute myocardial infarction. No. 11. Karger, Basel, pp. 180–184.

Larcan, A. and Stoltz, J. F. (1970) *Microcirculation et Hemorheologie*. Masson, Paris.

McIntire, L. V. (ed.) (1985) *Guidelines for Blood–Material Interactions*. Report of a National Heart, Lung, and Blood Institute Working Group. U. S. Dept. of HHS, PHS, and NIH. NIH Publication No. 85-2185.

McMillan, D. E. and Utterback, N. (1980) Maxwell fluid behavior of blood at low shear rate. *Biorheology* **17**, 343–354.

McMillan, D. E., Utterback, N. G., and Stocki, J. (1980) Low shear rate blood viscosity in diabetes. *Biorheology* **17**, 355–362.

Merrill, E. W., Cokelet, G. C., Britten, A., and Wells, R. E. (1963) Non-Newtonian rheology of human blood effect of fibrinogen deduced by "subtraction." *Circulation Res.* **13**, 48–55.

Merrill, E. W., Gilliland, E. R., Cokelet, G. R., Shin, H., Britten, A., and Wells, R. E. (1963) Rheology of human blood, near and at zero flow. *Biophys. J.* **3**, 199–213.

Merrill, W. E., Margetts, W. G., Cokelet, G. R., and Gilliland, E. W. (1965) The Casson equation and rheology of blood near zero shear. In *Symposium on Biorheology*, A Copley (ed.) Interscience Publishers, New York, pp. 135–143.

Merrill, E. W., Benis, A. M., Gilliland, E. R. Sherwood, R. K., and Salzman, E. W. (1965) Pressure-flow relations of human blood in hallow fibers at low flow rates. *J. Appl. Physiol.* **20**, 954–967.

Messmer, K. and Schmid-Schoenbein, H. (eds.) (1972) *Hemodilation: Theoretical Basis and Clinical Application*. Karger, Basel.

Oka, S. (1965) Theoretical considerations on the flow of blood through a capillary. In *Symposium on Biorheology*, A. L. Copley (ed.) Interscience, New York, pp. 89–102.

Oka, S. (1974) *Rheology–Biorheology*. Syokabo, Tokyo (in Japanese).

Phibbs, R. H. (1969) Orientation and distribution of erythrocytes in blood flowing through medium-sized arteries. In *Hemorheology*, A. C. Copley (ed.) Pergamon Press, New York, pp. 617–630.

Rand, R. P. and Burton, A. C. (1964) Mechanical properties of the red cell membrane. *Biophys. J.* **4**, 115–136.

Rand, P. W., Barker, N., and Lacombe, E. (1970) Effects of plasma viscosity and aggregation on whole blood viscosity. *Am. J. Physiol.* **218**, 681–688.

Rowlands, S., Groom, A. C., and Thomas, H. W. (1965) The difference in circulation times between erythrocyte and plasma in vivo. In *Symposium on Biorheology*, A. Copley, (ed.) Interscience Publishers, New York, pp. 371–379.

Scott-Blair, G. W. (1974) *An Introduction to Biorheology*. Elsevier, New York.

Thurston, G. B. (1972) Viscoelasticity of human blood. *Biophys. J.* **12**, 1205–1217.

Thurston, G. B. (1973) Frequency and shear rate dependence of viscoelasticity, of human blood. *Biorheology* **10**, 375–381; (1976) **13**, 191–199; (1978) **15**, 239–249; (1979) **16**, 149–162.

Thurston, G. B. (1976) The viscosity and viscoelasticity of blood in small diameter tubes. *Microvasc. Res.* 11, 133–146.

Vadas, E. B., Goldsmith, H. L., and Mason, S. G. (1973) The microrheology of colloidal dispersions. I. The microtube technique. *J. Colloid Interface Sci.* 43, 630–648.

Whitmore, R. L. (1968) *Rheology of the Circulation.* Pergamon Press, New York.

Yen, R. T. and Fung, Y. C. (1973) Model experiments on apparent blood viscosity and hematocrit in pulmonary alveoli. *J. Appl. Physiol.* 35, 510–517.

CHAPTER 4

Mechanics of Erythrocytes, Leukocytes, and Other Cells

4.1 Introduction

In the previous chapter, we studied the flow properties of blood. In this chapter, we turn our attention to the blood cells. We give most of the space to the red blood cells, but treat the white blood cells and other cells toward the end of the chpater.

Red blood cells are the gas exchange units of animals. They deliver oxygen to the tissues of all organs, exchange with CO_2, and return to the lung to unload CO_2 and soak up O_2 again. This is, of course, what circulation is all about. The heart is the pump, the blood vessels are the conduits, and the capillary blood vessels are the sites where gas exchange between blood and tissue or atmosphere takes place.

If one observes human red blood cells suspended in isotonic solution under a microscope, their beautiful geometric shape cannot escape attention (see Fig. 4.1:1; which shows two views of a red blood cell, one a plane view, and one a side view). The cell is disk-shaped. It has an almost perfect symmetry with respect to the axis perpendicular to the disk. The question is often asked: Why are human red cells so regular? Why are they shaped the way they are? When red cells grow in the bone marrow, they have nuclei, and their shape is irregular. Then as they mature, they expel their nuclei and enter the blood. They circulate in the body for 120 days or so, then swell into spherical shape and become hemolyzed by macrophages in the spleen.

In circulating blood, however, the red blood cells are severely deformed. Figure 4.1:2 shows photographs of blood flow in the capillary blood vessels in the mesentery of the rabbit and the dog. Note how different the cell shapes are compared with the isolated floating cells shown in Fig. 4.1:1! Some